AFCRL-65-668

MODAL ANALYSIS AND SYNTHESIS OF ELECTROMAGNETIC FIELDS

by

L. B. Felsen and N. Marcuvitz

Research Report No. PIBMRI-1257-65
Contract No. AF-19(628)-4324
Project No. 4600, Task No. 460004

for

Air Force Cambridge Research Laboratories
Office of Aerospace Research
United States Air Force
L. G. Hanscom Field
Bedford, Massachusetts

August 5, 1965

FOR
$3.00 0.75 70 as

MRI

POLYTECHNIC INSTITUTE OF BROOKLYN
MICROWAVE RESEARCH INSTITUTE
ELECTROPHYSICS DEPARTMENT

AFCRL-65-668

Research Report No. PIBMRI-1257-65
Contract No. AF-19(628)-4324

MODAL ANALYSIS AND SYNTHESIS OF ELECTROMAGNETIC FIELDS

by

L. B. Felsen and N. Marcuvitz

Polytechnic Institute of Brooklyn
Graduate Center
Route 110
Farmingdale, N. Y. 11735

Research Report No. PIBMRI-1257-65
Contract No. AF-19(628)-4324
Project No. 4600, Task No. 460004

August 5, 1965

Title Page
Abstract
Acknowledgement
Table of Contents
58 Pages of Text
1 Page of References
DD Form 1473

L. B. Felsen
Professor

N. Marcuvitz
Institute Professor

Prepared for

Air Force Cambridge Research Laboratories
Office of Aerospace Research
United States Air Force
Bedford, Massachusetts

The following report, to be issued at periodic intervals, is based upon material in Courses "Electromagnetic Radiation and Diffraction" and "Wave Propagation in Arbitrary Media", currently given at the Polytechnic Institute of Brooklyn. It is hoped that these notes will eventually appear in book form.

Abstract

After a general discussion of non-harmonic electromagnetic processes from the viewpoint of temporal Fourier (or Laplace) analysis and synthesis, a class of problems is considered for which the transient solution may be recovered in simple form. Included in this category are pulsed point, line and plane wave sources in free space, and in the presence of a) a dielectric half-space, b) a perfectly absorbing or perfectly conducting wedge or half plane, and c) a unidirectionally conducting infinite and semi-infinite screen. Explicit expressions for the transient response, found by a systematic application of the modal procedures discussed in earlier chapters in this sequence, are interpreted in physical terms. Attention is then given to a second class of problems wherein an electric charge moves uniformly along a straight trajectory in various environments. The associated radiation is now of the Cerenkov type, and formulas for the fields as well as the radiated power are given.

Acknowledgement

The work reported herein was sponsored by the Air Force Cambridge Research Laboratories, Office of Aerospace Research, United States Air Force, Bedford, Massachusetts, under Contract No. AF-19(628)-4324. The authors express their appreciation to Mrs. M. Bartoli for typing and proofreading the manuscript.

Table of Contents

CHAPTER VII - Radiation from Source Distributions with Non-Harmonic Time Dependence

	Page
Abstract	ii
Acknowledgement	iii
Table of Contents	iv
A. General Remarks	1
1. Modal analysis and synthesis in time	2
2. Inversion of certain problems in elementary form	7
B. Pulsed Sources in Free Space	10
1. Line source	10
2. Point source	12
3. Plane wave	12
C. Pulsed Sources in the Presence of a Dielectric Half-Space	13
1. Line source	13
2. Point source	16
D. Pulsed Sources in the Presence of a Wedge	21
1. Absorbing wedge	21
a. Line source excitation	21
b. Plane wave excitation	25
c. Point source excitation	26
2. Perfectly conducting wedge and half plane	27
a. Line source excitation	27
b. Plane wave or point source excitation	30
E. Pulsed Line Source in the Presence of a Unidirectionally Conducting Infinite and Semi-Infinite Screen	31
1. Infinite screen	31
2. Half plane	37
F. Radiation from Sources in Uniform Rectilinear Motion (Cerenkov-type effects)	43
1. General remarks	43

Table of Contents (continued)

	Page
2. Infinite dielectric medium	45
a. Circular waveguide representation	45
b. Rectangular waveguide representation	50
3. Two dielectric media separated by a plane interface	51
4. Anisotropic dielectric	55
a. Uniaxial anisotropy	55
b. Use of the refractive index diagram	56
Appendix A - The effect of pole singularities on the integration path	A1
References	viii

This report, which includes Chapter VII, is also a continuation of Reports R-446-55, R-726-59, R-776-59, 841-60, 1057-62, 1083-62, 1124-63, 1225-64 and 1243-64.

Report R-446-55(a) and (b) consist of:

Chapter I - Basic Concepts

Chapter II - Network Formalism in Uniform Waveguide

Appendix I - Derivation of the Transverse Field Equations

Report R-726-59 includes:

Chapter II, Appendix II - Field Representation in Uniform Waveguides with Inhomogeneously Filled Cross-Sections

Chapter III - Classical and Network Evaluation of Mode Functions

Report R-776-59 includes:

Chapter IV - Asymptotic Evaluation of Integrals

Appendix A - Asymptotic Expansion of $I(\Omega) = \int_P G(s)\, e^{\Omega \tau(s)} ds$

Report 841-60 includes:

Chapter I - Appendix - Fundamental Properties of the Electromagnetic Field

Chapter II - Section 9 - Modal Representations of the Dyadic Green's Functions in Longitudinally Stratified Regions

Chapter V - Part I - Radiation Problems in Plane Stratified Regions

Report 1057-62 includes:

Chapter V - Part II - Radiation Problems in Plane Stratified Regions

Appendix A - Approximate Boundary Conditions Representative of Highly Lossy, and of Certain Reactive Interfaces

Appendix B - Radiation Problems Involving Media with Negative Real Dielectric Constant

Chapter V - Problems

Report 1083-62 includes:

Chapter III - Addition to chapter

Chapter IV - Appendix C - continued

Chapter VI - Radiation Problems in Waveguides with Cross Sections Describable in Terms of Circular Cylindrical Coordinates

Appendix A - Asymptotic Formulas for $H_\nu^{(1)}(z)$ and $H_\nu^{(2)}(z)$

Appendix B - Miscellaneous Formulas Involving Cylinder Functions

Appendix C - Higher order terms in the asymptotic expansion of the diffraction field of a wedge

Report 1124-63 includes:

Chapter VIII - Radiation and Diffraction in Uniaxially Anisotropic Regions

Report 1225-64 includes:

Chapter III - Appendix A - Approximate Methods for Solving the Transmission Line Equations in Variable Media

Chapter V - Part III - Radiation Problems in Plane Stratified Regions

Chapter V - Appendix C - The Limit of Geometrical Optics

Report 1243-64 includes:

Chapter II - Appendix II - Field Representations in Arbitrary Uniform Waveguides

Chapter X - Radiation and Diffraction in Gyrotropic Regions

BLANK PAGE

CHAPTER VII

RADIATION FROM SOURCE DISTRIBUTIONS WITH NON-HARMONIC TIME DEPENDENCE

A. General Remarks

As noted in Chapter I, the modal viewpoint may be applied consistently to the study of time and space dependent fields through the use of an appropriate representation. The time dependence, which enters into the Maxwell field equations via the derivative operator $(\partial/\partial t)$, may be eliminated by a representation in terms of eigenfunctions $\exp(j\omega t)$, and the resulting reduced equations are descriptive of the time-harmonic field. Chapters V and VI have been concerned with the detailed study of boundary value problems arising from excitation by time-harmonic (steady-state) source configurations in various environments. While this suffices for many practical situations wherein the source function is either continuously sinusoidal or pulsed, with the pulse width much greater than a sinusoidal period, occasions arise when these conditions are not satisfied and when a transient analysis is essential. From a theoretical viewpoint, an understanding of transient processes provides further insight into the mechanism of propagation and diffraction since it is then possible to track the progress of an electromagnetic disturbance in time and space.

As shown by the analysis in Chapter I, the transient response to a source with non-harmonic temporal variation may be synthesized by a continuous superposition of modal, time-harmonic fields. The relevant modal index is the frequency variable ω, and the resulting Fourier integral operates on the solutions accounting for the spatial aspects of the problem. Since the latter may also involve single or double integrations (see Chapters V and VI), the expressions for the space-time dependent field are generally quite involved. As in the time-harmonic case where asymptotic methods have been found useful to produce simple formulas for the radiation field (i.e., the field at large distances or at short wavelengths), it is desirable now to look for approximations valid in certain time intervals. As shown in the discussion below, there exists an intimate relation between the time-harmonic field at high frequencies and the transient field near the time of arrival of the first response. Thus, many of the asymptotic results obtained in Chapters V and VI may be easily transcribed to furnish the field behavior in the vicinity of an impinging wave front under transient conditions.

It will also be shown that certain time-harmonic solutions may be inverted exactly in simple form, thereby furnishing elementary results for pulse propagation and diffraction problems valid at all observation times. The physical implications of these solutions provide further understanding of propagation and diffraction processes under rather general conditions.

1. Modal analysis and synthesis in time

By the procedure described in Chapter I, one represents a temporal source function in terms of its time-harmonic constituents, evaluates the harmonic steady-state response, and finally obtains the transient field behavior as a modal superposition of the steady-state solutions. In mathematical terms, one takes the Fourier transform of the time-dependent, inhomogeneous Maxwell field equations, solves the resulting steady-state equations, and recovers the temporal response by applying the inverse Fourier transform. Let $\hat{f}(\underline{r}, t)$ denote a real space-time dependent function, and $f(\underline{r}, \omega)$ its Fourier spectrum; then $\hat{f}$ and f are related via the Fourier transform pair

$$f(\underline{r}, \omega) = \int_{-\infty}^{\infty} \hat{f}(\underline{r}, t)\, e^{-j\omega t} dt \quad , \tag{1a}$$

$$\hat{f}(\underline{r}, t) = \frac{1}{2\pi} \int_{-\infty}^{\infty} f(\underline{r}, \omega)\, e^{j\omega t} d\omega \quad , \tag{1b}$$

provided that $\int_{-\infty}^{\infty} |\hat{f}|\, dt$ exists (see also Eq. (95)). If the electric and magnetic current source distributions $\hat{\underline{j}}(\underline{r}, t)$ and $\hat{\underline{j}}_m(\underline{r}, t)$, respectively, are stationary in space and have a prescribed time dependence, they can be represented in the separable form

$$\hat{\underline{j}}(\underline{r}, t) = \underline{J}(\underline{r})\, \hat{g}(t) \quad , \qquad \hat{\underline{j}}_m(\underline{r}, t) = \underline{J}_m(\underline{r})\, \hat{h}(t) \quad , \tag{2}$$

and their transforms are

$$\underline{j}(\underline{r}, \omega) = \underline{J}(\underline{r})\, g(\omega) \quad , \qquad j_m(\underline{r}, \omega) = \underline{J}_m(\underline{r})\, h(\omega) \quad . \tag{3}$$

In this instance, the space-time dependent electromagnetic fields are given in terms of the solutions $\underline{E}(\underline{r}) \equiv \underline{E}(\underline{r}, \omega)$ and $\underline{H}(\underline{r}) \equiv \underline{H}(\underline{r}, \omega)$ of the steady-state Maxwell field

equations (2.1) by

$$\hat{\underline{E}}(\underline{r}, t) = \frac{1}{2\pi} \int_{-\infty}^{\infty} \left[\underline{E}^J(\underline{r}, \omega)\, g(\omega) + \underline{E}^M(\underline{r}, \omega)\, h(\omega) \right] e^{j\omega t} d\omega \quad , \tag{4a}$$

$$\hat{\underline{H}}(\underline{r}, t) = \frac{1}{2\pi} \int_{-\infty}^{\infty} \left[\underline{H}^J(\underline{r}, \omega)\, g(\omega) + \underline{H}^M(\underline{r}, \omega)\, h(\omega) \right] e^{j\omega t} d\omega \quad , \tag{4b}$$

where $\underline{E}^J$ ($\underline{H}^J$) and $\underline{E}^M$ ($\underline{H}^M$) are the electric (magnetic) fields due to the electric and magnetic current excitations, respectively. In utilizing the steady-state solutions $\underline{E}(\underline{r}, \omega)$ and $\underline{H}(\underline{r}, \omega)$ in (4a, b), one should attend to the fact that ω ranges from $-\infty$ to $+\infty$. Hence, a steady-state solution obtained for an assumed dependence $\exp(+j\omega t)$, $\omega \geq 0$, can be employed only in the interval $0 \leq \omega < \infty$; in the interval $-\infty < \omega \leq 0$, one must utilize the solution appropriate to $\exp(-j\omega t)$, $\omega > 0$. These remarks are of special significance for radiation problems in unbounded regions where the form of the time-harmonic fields satisfying a radiation condition is linked intimately to the assumed time dependence $\exp(+j\omega t)$ or $\exp(-j\omega t)$ (for an alternative formulation involving positive frequencies only, see Eq. (95)).

An important special class of source distributions is characterized by functions which vanish prior to some given time reference, say $t = 0$. If the electromagnetic fields are likewise assumed to be zero when $t < 0$, the integral in (1a) defining all relevant Fourier transforms extends from only $t = 0$ to $t = \infty$. In this instance, it is frequently more convenient to employ instead of the Fourier integral representation the Laplace transform

$$\bar{f}(\underline{r}, s) = \int_{0}^{\infty} \hat{f}(\underline{r}, t)\, e^{-st} dt \tag{5a}$$

since one then extends substantially the range of representable functions. The parameter s in (5a) is chosen so that $(\mathrm{Re}\ s) \geq s_o$, where $s_o > 0$ is the lowest value of $(\mathrm{Re}\ s)$ to assure the absolute convergence of the integral. The existence of the integral representation for $\bar{f}(\underline{r}, s)$ implies that of the inverse transformation

$$\hat{f}(\underline{r}, t) = \frac{1}{2\pi j} \int_{s_o - j\infty}^{s_o + j\infty} \bar{f}(\underline{r}, s)\, e^{st} ds \quad , \tag{5b}$$

with $\hat{f} \equiv 0$ for $t < 0$. Since from Eq. (5a), $\bar{f}$ is an analytic function of s when $\mathrm{Re}\ s \geq s_o$, the validity of the last statement (causality) can be verified by completing the integration path with a semicircle at infinity in the right half of the s-plane and

invoking the Cauchy integral formula. Upon comparing Eqs. (1a) and (5a), one notes that

$$\bar{f}(\underline{r}, s) = f(\underline{r}, -js) \quad , \quad (\mathrm{Re}\ s) > s_o \quad , \tag{5c}$$

i.e., the Laplace transform $\bar{f}$ can be inferred from the steady-state solution f appropriate to a time dependence $\exp(j\omega t)$, $\omega > 0$ by analytic continuation of the real frequency variable ω into the complex domain $\omega = -js$, $(\mathrm{Re}\ s) > s_o$. For source distributions satisfying Eqs. (2), the field response can be represented as in Eqs. (4a, b), with the above-noted change of variable to s and use of the integration contour in Eq. (5b).

Since the Laplace inversion in Eq. (5b) cannot generally be carried out in closed form (an exception occurs for the class of problems discussed below), it is useful to call attention to an asymptotic equivalence between the time-harmonic solution at high frequency $(s \to \infty)$ and the transient solution near the time of arrival $t_o > 0$ of the first response at a given observation point $\underline{r}$. Writing $\hat{f}(\underline{r}, t)$ for a typical field component, one has

$$\bar{f}(\underline{r}, s) = \int_{t_o}^{\infty} \hat{f}(\underline{r}, t)\, e^{-st} dt = e^{-st_o} \int_{o}^{\infty} \hat{f}(\underline{r}, \xi + t_o) e^{-s\xi}\, d\xi \quad , \tag{6a}$$

since $\hat{f} = 0$ for $t < t_o$. The principal contribution to the integral for large s arises from the vicinity of the origin $\xi = 0$ (see also Chapter IV). If $\hat{f}$ behaves near $t = t_o$ according to

$$\hat{f}(\underline{r}, t) \sim \xi^{a}(d_o + d_1\xi + d_2\xi^2 + \ldots) + d'\delta(\xi) \quad , \quad \mathrm{Re}\ a > -1 \quad , \quad \xi = t - t_o \quad , \tag{6b}$$

where the d_i and d' depend on $\underline{r}$ only, then the behavior of $\bar{f}$ for large s is obtained upon substitution into Eq. (6a), interchange of the orders of integration and summation, and use of the definition of the gamma function (see Eq. (4.47)),

$$\bar{f}(\underline{r}, s)\, e^{st_o} \sim d' + \sum_{n=0}^{\infty} \frac{d_n}{s^{a+n+1}} \Gamma(a+n+1) \quad , \quad s \to \infty \quad . \tag{6c}$$

Thus, the leading coefficients in the expansion for $\hat{f}$ are given by

$$d_o = \lim_{s \to \infty} \frac{\left[\bar{f}(\underline{r}, s)\, e^{st_o} - d'\right] s^{a+1}}{\Gamma(a+1)} \quad ,$$

$$d_1 = \lim_{s \to \infty} \left[\frac{\left(\bar{f}(\underline{r}, s)\, e^{st_o} - d'\right) s^{a+2}}{\Gamma(a+2)} - \frac{s d_o}{a+1} \right] \quad , \tag{6d}$$

etc. Conversely, the response immediately after the arrival of a given field constituent (for example, the direct, reflected, or diffracted field) determines the time-harmonic behavior of the corresponding constituent in the high-frequency limit. With $s = j\omega$ and $\alpha = 0$, the series (6c) yields a high-frequency asymptotic expansion of the steady-state field, the first term of which represents the geometric-optical approximation (see Chapter V, Appendix C).* The amplitude of the geometric-optical field and of the impulsive constituent of the transient response are therefore both specified by $d'(\underline{r})$. Since $\hat{f} \equiv 0$ for $\xi < 0$, the d_i coefficients in the series (6b) (if $\alpha = 0$ and $d' = 0$) describe the regularity properties of $\hat{f}$ at $\xi = 0$. Thus, if $d_0 \ldots d_N = 0$, $\hat{f}$ and its derivatives up to order N are continuous at $\xi = 0$ and the resulting asymptotic behavior as $\omega \to \infty$ is $O(\omega^{-N-1})$. The high-frequency dependence is therefore indicative of the discontinuities in the function $\hat{f}$ or its derivatives at the time of arrival of the first response.[1]

For observation times long after the arrival of the first response, $\xi \gg 1$, an evaluation of the inverse Laplace transform in Eq. (5b) may be attempted by deforming the integration contour about the singularities of $\bar{f}(\underline{r}, s)$ in the half plane $\mathrm{Re}\, s < 0$. In view of the presence of the exponential $\exp(s\xi)$, only those singularities with small $(\mathrm{Re}\, s)$ are significant and may form the basis for an effective approximation of the time dependent function $\hat{f}(\underline{r}, t)$.

As in the case of time-harmonic problems, the transient field response to non-harmonic source distributions in plane stratified regions can be evaluated through the use of auxiliary potential functions. In particular, Eqs. (2.18) involving the E and H mode Hertzian potentials $\hat{\Pi}'(\underline{r}, t)$ and $\hat{\Pi}''(\underline{r}, t)$, respectively, apply also in this case provided that $(j\omega)$ is replaced by the differential operator $(\partial/\partial t)$. It is to be noted that for media with dielectric losses, characterized in the steady-state by a complex dielectric constant $\epsilon = \epsilon_r - j\sigma/\omega$, σ = conductivity, $j\omega\epsilon$ is replaced by the operator $[\epsilon_r(\partial/\partial t) + \sigma]$. Similar remarks apply to materials having magnetic losses. Unless mentioned otherwise, the media are henceforth assumed to be lossless, and ϵ_r is taken to be frequency independent.

It is sometimes more convenient to deal not with the source current densities $\hat{\underline{j}}$ and $\hat{\underline{j}}_m$, but rather with the dipole moment densities $\hat{\underline{p}}$ and $\hat{\underline{m}}$ defined as

$$\hat{\underline{j}}(\underline{r}, t) = \frac{\partial}{\partial t}\hat{\underline{p}}(\underline{r}, t) \quad , \qquad \hat{\underline{j}}_m(\underline{r}, t) = \frac{\partial}{\partial t}\hat{\underline{m}}(\underline{r}, t) \quad . \tag{7}$$

*Fractional values of α, resulting in fractional powers of ξ in Eq. (6b) and s in Eq. (6c), are required to describe diffracted fields (see Sec. D).

For example, the radiation from a longitudinally directed electric or magnetic current element having a dipole moment

$$\hat{\underline{p}}(\underline{r}, t) = \underline{z}_o \delta(\underline{r}-\underline{r}') \hat{q}(t) \quad , \qquad \hat{\underline{m}}(\underline{r}, t) = \underline{z}_o \delta(\underline{r}-\underline{r}') \hat{q}_m(t) \quad , \tag{7a}$$

respectively, can be determined via Eqs. (2.80) as

$$\hat{\underline{E}}(\underline{r}, t) = \frac{1}{\epsilon}(\nabla \times \nabla \times \underline{z}_o) \hat{G}'(\underline{r}, \underline{r}';t) - (\nabla \times \underline{z}_o) \frac{\partial}{\partial t} \hat{G}''(\underline{r}, \underline{r}';t) \quad , \tag{8a}$$

$$\hat{\underline{H}}(\underline{r}, t) = (\nabla \times \underline{z}_o) \frac{\partial}{\partial t} \hat{G}'(\underline{r}, \underline{r}';t) + \frac{1}{\mu}(\nabla \times \nabla \times \underline{z}_o) \hat{G}''(\underline{r}, \underline{r}';t) \quad , \tag{8b}$$

where $\hat{G}'$ and $\hat{G}''$ are the temporal functions corresponding to the spectrum functions $G'(\underline{r}, \underline{r}';\omega)\, q(\omega)$ and $G''(\underline{r}, \underline{r}';\omega)\, q_m(\omega)$, respectively. G' and G'' are the scalar Green's functions defined in Eqs. (2.82) and (2.83), respectively.* Retention of the current densities leads to a somewhat more complicated formulation requiring via Eq. (3) the inversion of a spectrum function $G'g/\omega$, etc.

It has been shown in Chapters V and VI that the time-harmonic high-frequency field** may be interpreted in terms of rays which define the trajectories of energy flow. The ray picture is even more relevant in the transient case where the propagation of the disturbance (described by a family of wave fronts), and the associated flow of energy (along the rays, the orthogonal trajectories to the family of wave fronts in isotropic regions), may be tracked in time and space. The electromagnetic fields and (or) some of their derivatives are discontinuous across a wave front, and the determination of the progress of the front is equivalent to the study of the field singularities in time and space.[1] From a transient analysis in the presence of boundaries or obstacles (see problems in the remainder of this Chapter), it becomes clear how the incident wave front, after reaching the boundary, is reflected, refracted or diffracted, and how the propagation of the reflected, refracted or diffracted wave fronts may be characterized in terms of rays.

In view of the remarks following Eqs. (6), there exists an intimate relation between the time-harmonic, high-frequency field and the transient solution in the immediate vicinity of the time of arrival of the first response. In this manner, the use of rays and of the associated phase fronts carries over naturally into the interpretation

---

* ϵ and μ in these equations have been treated as (frequency-independent) constants.

** In the asymptotic calculations in Chapters V and VI, the distance D from the source has often been introduced as the large parameter. Since the distance always occurs in the dimensionless combination kD, the results apply as well when k is large and D is moderate. This latter interpretation is relevant for the present discussion.

of steady-state phenomena at high frequencies.[1]

This sequence has been reversed in the present volume where, in keeping with the modal viewpoint, the time-harmonic case has been considered first. Since the ray interpretation of time-harmonic high-frequency fields has been emphasized in connection with various problems in Chapters V and VI, the interpretation of the corresponding transient solutions in this Chapter is carried out only briefly, with reference to the earlier steady-state results.

In view of the preceding remarks, it should not be difficult for the reader to relate the previously derived ray solutions to the present discussion of transient fields. While it should be clear that the high-frequency asymptotic results for the time-harmonic field may be easily transcribed to yield the transient field near the time of arrival of the first response, the discussion below is confined to a necessarily more restricted class of problems for which one may construct simple transient solutions valid at <u>all</u> observation times. These results show the variation of the response characteristics as time elapses after the passing of the initial wave front.

2. Inversion of certain problems in elementary form

While the temporal response function $\hat{f}$ must in general be recovered from its Laplace transform $\bar{f}$ by performing the integration in Eq. (5b), this procedure can be circumvented in certain cases if one is able to cast the transform solution into a representation as in Eq. (5a), from which the temporal function is obtained by inspection. More generally, one seeks to represent the transform solution in the form

$$\bar{f}(\underline{r}, s) = a(s)\,\bar{g}(s)\,h(\underline{r}, s) \quad , \tag{9}$$

$$h(\underline{r}, s) = \int_0^\infty e^{-s\tau} A(\underline{r}, \tau)\,d\tau \quad , \tag{9a}$$

where $\bar{g}(s)$ is the transform of the prescribed source function $\hat{g}(t)$ ($\hat{g} = 0$ for $t \leq 0$), $a(s)$ is a polynomial in s, and A is a function of $\underline{r}$ and the real integration variable τ, but not of s. Comparison of Eqs. (5a) and (9a) shows that $A(\underline{r}, t)$ is the time function having a spectrum $h(\underline{r}, s)$, i.e.,

$$h(\underline{r}, s) \rightarrow A(\underline{r}, t) \quad . \tag{10a}$$

Since the operation $a(d/dt)$ in the time domain implies multiplication by $a(s)$ in the transform domain, one has

$$a(s)\,\bar{w}(s) \rightarrow a(d/dt)\,\hat{w}(t) \quad , \tag{10b}$$

while, from the convolution theorem,

$$\bar{u}(s)\,\bar{w}(s) \rightarrow \int_0^t u(\alpha)\,w(t-\alpha)\,d\alpha = \int_0^t u(t-\alpha)\,w(\alpha)\,d\alpha \quad . \tag{10c}$$

Hence, Eq. (9) can be inverted by inspection to yield

$$\hat{f}(\underline{r},t) = a\left(\frac{d}{dt}\right)\int_0^t \hat{g}(\alpha)\,A(\underline{r},t-\alpha)\,d\alpha = a\left(\frac{d}{dt}\right)\int_0^t \hat{g}(t-\alpha)\,A(\underline{r},\alpha)\,d\alpha \quad , \qquad t>0 \quad . \tag{11}$$

It has been assumed above that the system is quiescent when $t \leq 0$ so that there is no contribution from initial value terms at $t = 0$. If $a(d/dt)\,\hat{g}(t) = \delta(t-t')$, i.e., the source function (or its derivatives(s) if the function "a" is not a constant) is impulsive, the solution is given directly by $A(\underline{r}, t-t')$.

It is to be expected that only a limited class of problems yields transforms which can be expressed as in Eq. (9), in view of the special representation for h required in Eq. (9a). Included in this category are those time-harmonic solutions which are expressible in terms of the integral representation [2]

$$L(\gamma,\varpi,\omega) = \int_{\hat{P}} e^{-jk\gamma\cos(w-\varpi)}\,u(w)\,dw \qquad (e^{j\omega t}\text{ dependence}) \tag{12a}$$

or

$$L(\gamma,\varpi,\omega) = \int_{\bar{P}} e^{ik\gamma\cos(w-\varpi)}\,u(w)\,dw \qquad (e^{-i\omega t}\text{ dependence}) \quad , \tag{12b}$$

where the contours of integration $\hat{P}$ and $\bar{P}$ are those in Figs. 5.5(b) and 5.6(b), respectively. The parameters γ and ϖ are assumed to be positive, with ϖ restricted to the range $0<\varpi<\pi/2$, and the function $u(w)$ is independent of $k = \omega/c$, where $c = (\mu\varepsilon)^{-1/2}$ is the speed of light in the medium. As observed in Chapters V and VI, a number of time-harmonic diffraction problems can be expressed in this form. Upon letting $\omega \rightarrow -js$ in Eq. (12a), one may write

$$\bar{L}(\gamma,\varpi,s) = \int_{-j\infty}^{j\infty} e^{-s(\gamma/c)\cos w}\,u(w+\varpi)\,dw \quad , \tag{13}$$

where it has been assumed that the function $u(w)$ has no singularities in the strip $0<|\mathrm{Re}\,w|<\pi/2$ (if such singularities are present, their effect may lead to additional contributions to $\bar{L}$), and the positive parameter s is large enough to assure convergence of the integral. Since $\exp[-s(\gamma/c)\cos(w-\varpi)]$ decays in the strip $\cos(w_r-\varpi)>0$, the contour of integration can be shifted to achieve the representation (13) (see Fig. 5.4).

The successive changes of variable $\beta = -jw$ and $\tau = (\gamma/c)\cosh\beta$ lead to the formulation

$$\bar{L}(\gamma, \varphi, s) = j\int_{\frac{\gamma}{c}}^{\infty} e^{-s\tau} \frac{b(\tau)}{\sqrt{\tau^2 - \left(\frac{\gamma}{c}\right)^2}}\, d\tau \quad , \tag{14a}$$

where

$$b(\tau) = u\left[\varphi + j\cosh^{-1}\left(\frac{c\tau}{\gamma}\right)\right] + u\left[\varphi - j\cosh^{-1}\left(\frac{c\tau}{\gamma}\right)\right] \quad . \tag{14b}$$

Eq. (14a) is evidently in the form (9a), with

$$A(\tau) = \begin{cases} 0 & , \quad \tau < \frac{\gamma}{c} \\ \dfrac{jb(\tau)}{\sqrt{\tau^2 - \frac{\gamma^2}{c^2}}} & , \quad \tau > \frac{\gamma}{c} \end{cases} \quad . \tag{15}$$

If $v(w) = ju(w)$ is real for real values of w, then $v(w^*) = v^*(w)$ (from the Schwartz reflection principle) and $b(\tau)$ can be written as

$$jb(\tau) = 2\,\mathrm{Re}\left\{ju\left[\varphi + j\cosh^{-1}\left(\frac{c\tau}{\gamma}\right)\right]\right\} \quad . \tag{15a}$$

Several applications of this result are given in the following sections. (The preceding considerations also apply to the $\exp(-i\omega t)$ formulation in Eq. (12b) provided that $j \to -i$.)

It should be emphasized that the formulation in Eq. (14a) is useful even when $u(w)$ is dependent on s. Although one cannot then perform the Laplace inversion in closed form, an expansion of $u(w;s)$ in series of powers of $(1/s)$ or s permits the simple derivation of asymptotic results in the time domain applicable immediately and long after the arrival of the first response, respectively.

B. Pulsed Sources in Free Space

1. Line source

Consider an infinite line source along the z-axis of a cylindrical coordinate system, characterized by the impulsive electric dipole moment distribution

$$\hat{\underline{p}}(\underline{r}, t) = \underline{z}_o \delta(\underline{\rho}) \hat{q}(t) \quad ; \quad \hat{q}(t) = 0 \quad , \quad t < 0 \quad . \tag{16}$$

Since $\hat{\underline{m}} \equiv 0$, and hence $\hat{G}'' = 0$, the evaluation of $\hat{G}'$ only is required for the determination of the electromagnetic fields from Eqs. (8).* From Eqs. (5.57), one has for an assumed $\exp(j\omega t)$ time dependence:

$$G'(\underline{\rho}, \underline{\rho}'; \omega) = -\frac{j}{4} H_o^{(2)}(k\rho) \quad , \quad k = \omega\sqrt{\mu\varepsilon} = \frac{\omega}{c} > 0 \quad , \tag{17}$$

which has the contour integral representation (see Eq. (5.60)),

$$G'(\underline{\rho}, \underline{\rho}'; \omega) = -\frac{j}{4\pi} \int_{\hat{P}} e^{-jk\rho \cos w} dw \quad . \tag{18}$$

Comparison with Eq. (12a) shows that $u(w) = -j/4\pi$ so that from Eq. (15)

$$A(\tau) = \begin{cases} 0 & , \quad \tau < \frac{\rho}{c} \\ \dfrac{1}{2\pi\sqrt{\tau^2 - \left(\frac{\rho}{c}\right)^2}} & , \quad \tau > \frac{\rho}{c} \end{cases} \quad . \tag{19}$$

The desired temporal function $\hat{G}'$ in Eq. (8), requiring the inversion of the spectrum function $\bar{G}'(\underline{\rho}, \underline{\rho}'; s)\,\bar{q}(s)$, is then written down directly from Eqs. (11) and (19):

$$\hat{G}'(\underline{\rho}, \underline{\rho}'; t) = \begin{cases} \dfrac{1}{2\pi} \displaystyle\int_{\rho/c}^{t} \hat{q}(t-a) \frac{1}{\sqrt{a^2 - \frac{\rho^2}{c^2}}} da & , \quad t > \frac{\rho}{c} \quad (20a) \\ 0 & , \quad t < \frac{\rho}{c} \quad . \quad (20b) \end{cases}$$

The electromagnetic fields can now be calculated by inserting $\hat{G}'$ from Eq. (20) into Eqs. (8).

---

* For this two-dimensional problem, $\underline{r} \equiv \underline{\rho}$, $(\partial/\partial z) \equiv 0$. Hence, $\hat{\underline{E}} = -\underline{z}_o \frac{1}{\varepsilon} \nabla^2 \hat{G}'$, etc.

It is of interest to examine the special case of an impulsive moment distribution $\hat{q}(t) = \delta(t-t')$, $t' > 0$. In this case Eqs. (20) yield

$$\hat{G}' = \begin{cases} \dfrac{1}{2\pi} \dfrac{1}{\sqrt{(t-t')^2 - \dfrac{\rho^2}{c^2}}} , & t > t' + \dfrac{\rho}{c} \quad (21a) \\ 0 , & t < t' + \dfrac{\rho}{c} , \quad (21b) \end{cases}$$

a result which could also have been written down directly from Eq. (19). Thus, the impulse at $t = t'$ creates a cylindrically symmetrical disturbance spreading outward from the source with velocity c and reaching an observation point ρ at a time $t = t' + \rho/c$. Although the action of the source is confined to the instant $t = t'$, a response of decreasing intensity persists at ρ after the passing of the initial wave front (Fig. 1(a)). (The reader may wish to construct the solution $\hat{G}' \approx \left(2\pi\sqrt{2\rho/c}\right)^{-1}(t-t'-\rho/c)^{-1/2}$ when $(t-t') \approx \rho/c$ directly from the asymptotic formula (5.37) and Eqs. (6)).

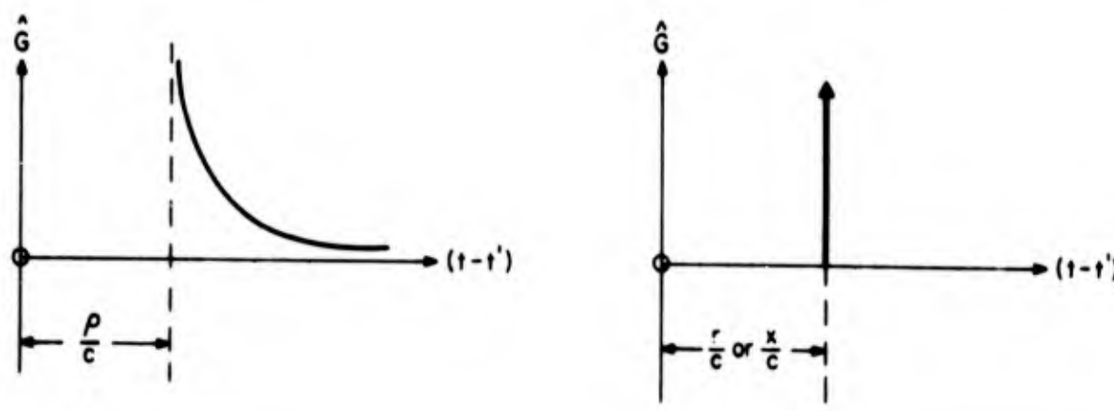

a) line source

b) point source or plane wave

Fig. 1 - Impulsive line source, point source and plane wave response observed at a distance ρ, r, and x, respectively.

2. Point source

A dipole in an infinite lossless medium is assumed to be characterized by the vector moment

$$\hat{\underline{p}}(\underline{r}, t) = \underline{z}_o \, \delta(\underline{r}) \, \hat{q}(t) \quad ; \quad \hat{q}(t) = 0 \quad , \quad t < 0 \quad . \tag{22}$$

The steady-state free-space Green's function is given in this case by

$$G'(\underline{r}, \underline{r}'; \omega) = \frac{e^{-jkr}}{4\pi r} \quad , \quad k = \frac{\omega}{c} \quad (e^{+j\omega t} \text{ dependence}) \tag{23a}$$

whence

$$\bar{G}'(\underline{r}, \underline{r}'; s) = \frac{e^{-sr/c}}{4\pi r} \quad , \quad \text{Re } s > 0 \quad . \tag{23b}$$

Since Eq.(23b) exhibits directly the form of Eq. (9a), with $A(\underline{r}, \tau) = (1/4\pi r)\,\delta(\tau - r/c)$, one obtains from Eq. (11) the temporal function corresponding to $\bar{G}'\bar{q}$:

$$\hat{G}'(\underline{r}, \underline{r}'; t) = \begin{cases} \dfrac{\hat{q}\left(t - \frac{r}{c}\right)}{4\pi r} \quad , & t > \dfrac{r}{c} \quad (24a) \\ 0 \quad , & t < \dfrac{r}{c} \quad . \quad (24b) \end{cases}$$

In this instance, the (scalar) disturbance is spherically symmetric about the source, propagates outward with velocity c and has at r a functional dependence on time identical with that at the source. In particular, when $\hat{q}(t) = \delta(t-t')$, the result in Eq. (24a) yields the three-dimensional free-space Green's function for the operator $\left(\nabla^2 - \partial^2/c^2\partial t^2\right)$ (Fig. 1(b)).

3. Plane wave

If the incident field is in the form of a plane wave propagating along the x-direction, the steady-state behavior for the $\exp(j\omega t)$ variation is expressed in terms of the potential function $G = \exp(-jkx)$. Since the k-dependence in this expression is the same as in Eq. (23a), it is concluded that if the field at some particular location, say $x = 0$, is described by the time function $\hat{q}(t)$, the temporal response is unchanged at another observation coordinate and is given by $\hat{q}\left(t - \frac{x}{c}\right)$. In particular, the propagation of an impulsive plane wave is characterized by the potential function (see Fig. 1(b)),

$$\hat{G}(x, t) = \delta\left(t - \frac{x}{c}\right) \quad . \tag{25}$$

C. Pulsed Sources in the Presence of a Dielectric Half-Space

This class of problems reveals how the previously determined transient fields in an unbounded medium are modified when a plane interface is present which separates two semi-infinite regions with different dielectric properties. It is found that the boundary gives rise to a reflected field whose amplitude is weighted by an appropriate measure of the plane wave reflection coefficient. Refracted and diffracted fields are also present but are described in a more complicated form which is not pursued here. To permit the recovery of explicit formulas for the response to line source and dipole excitation, the dielectrics are assumed to be independent of frequency. The line source calculation is straightforward and leads to a simple result, but considerable difficulty arises in the dipole case when neither the source point nor the observation point is located on the interface. Nevertheless, it is possible to derive a compact expression even for the latter configuration, as shown below.

1. Line source

The configuration of an infinite line source of electric current located at $\underline{\rho}' = (y', z')$ in the presence of a semi-infinite dielectric medium has been schematized in Fig. 5.16. We shall assume a dipole mement distribution as in Eq. (16),

$$\hat{\underline{p}}(\underline{r}, t) = \underline{x}_o \, \delta(\underline{\rho}-\underline{\rho}') \, \hat{q}(t) \quad , \qquad \underline{\rho}' = (0, z') \quad , \qquad z' < 0 \quad . \tag{26}$$

As noted there, the fields radiated by this source distribution are independent of x, with the electric field having only a single component $\hat{E}_x(\underline{r}, t)$ which can be inferred from the scalar Green's function $\hat{G}'$ [cf. Eq. (8a)] as

$$\hat{E}_x(\underline{r}, t) = -\frac{1}{\epsilon} \nabla^2 \hat{G}'(\underline{\rho}, \underline{\rho}'; t) \quad , \qquad (\partial/\partial x) \equiv 0 \quad . \tag{27a}$$

Similarly, for the magnetic field,

$$\hat{\underline{H}}(\underline{r}, t) = (\nabla \times \underline{x}_o) \frac{\partial}{\partial t} \hat{G}'(\underline{\rho}, \underline{\rho}'; t) \quad . \tag{27b}$$

In this section, the symbol $\underline{\rho}$ rather than $\hat{\underline{\rho}}$ (cf. Sec. 5.C.3) will be employed to denote the location of the point (y, z). Note that the coordinate designation has been changed from that in Sec. B1 to facilitate the direct use of the steady-state Green's function derived in Sec. 5.C.3.

In medium I of Fig. 5.16 ($z<0$), the steady-state Green's function $G'(\underline{\rho}, \underline{\rho}';\omega)$ given in Eq. (5.112a), comprises two terms: the free-space Green's function G_{f_1} for an infinite medium with constants ϵ_1, μ_1, and a secondary part G_s. The free-space Green's function has been evaluated in Eqs. (20), with ρ interpreted as the distance $|\underline{\rho}-\underline{\rho}'|$ from the source location. A suitable modal representation for G_s is given in Eq. (5.115) which is repeated for convenience:

$$G_s(\underline{\rho}, \underline{\rho}';\omega) = \frac{-j}{4\pi} \int_{\hat{P}} e^{-jk_1 R \cos(w-\varphi)} \Gamma(w)\, dw \quad , \tag{28}$$

where $k_1 = \omega/c_1 = \omega\sqrt{\mu\epsilon_1}$, $(y-y') = R \sin\varphi$, $|z+z'| = R\cos\varphi$, and

$$\Gamma(w) = \frac{\cos w - \sqrt{\epsilon - \sin^2 w}}{\cos w + \sqrt{\epsilon - \sin^2 w}} \quad , \qquad \epsilon = \frac{\epsilon_2}{\epsilon_1} = \frac{c_1^2}{c_2^2} \quad , \quad \mu_1 = \mu_2 = \mu \quad . \tag{28a}$$

If ϵ is assumed to be real and independent of frequency*, Eq. (28) is of the form (12a) and can therefore be inverted via Eq. (15). To assure that $\Gamma(w)$ has no singularities in the interval $0<|\mathrm{Re}\, w|<\pi/2$, ϵ is restricted to be larger than unity. Thus,

$$A(\tau) = \begin{cases} 0 \quad , & \tau < \dfrac{R}{c_1} \quad , \qquad (29a) \\[2ex] \dfrac{1}{2\pi\sqrt{\tau^2 - \dfrac{R^2}{c_1^2}}}\, \mathrm{Re}\, \Gamma\left[\varphi + j \cosh^{-1}\left(\dfrac{c_1\tau}{R}\right)\right] \quad , & \tau > \dfrac{R}{c_1} \quad , \qquad (29b) \end{cases}$$

---

*This assumption is valid if the frequency spectrum of the source is negligible in the vicinity of the atomic resonant frequencies of the medium.

and, from Eq. (11):

$$\hat{G}'_s(\underline{\rho}, \underline{\rho}'; t) = \frac{1}{2\pi} \int_{R/c_1}^{t} \hat{q}(t-a) \frac{\mathrm{Re}\, \Gamma\left[\varphi + j \cosh^{-1}\left(\frac{a c_1}{R}\right)\right]}{\sqrt{a^2 - \frac{R^2}{c_1^2}}} \, da \quad , \qquad t > \frac{R}{c_1} \qquad (30a)$$

$$0 \quad , \qquad t < \frac{R}{c_1} \quad . \qquad (30b)$$

For an impulsive moment distribution $\hat{q}(t) = \delta(t-t')$, $t' > 0$, Eqs. (30) reduce to

$$\hat{G}_s(\underline{\rho}, \underline{\rho}'; t) = \frac{1}{2\pi} \frac{\mathrm{Re}\, \Gamma\left[\varphi + j \cosh^{-1}\left(\frac{c_1 t - c_1 t'}{R}\right)\right]}{\sqrt{(t-t')^2 - \frac{R^2}{c_1^2}}} \quad , \qquad t > t' + \frac{R}{c_1} \qquad (31a)$$

$$0 \quad , \qquad t < t' + \frac{R}{c_1} \quad . \qquad (31b)$$

Hence, the field due to an impulsive source located at $(0, z')$, $z' < 0$, observed at the observation point (y, z), $z < 0$, comprises the direct wave as in Eq. (20), plus a reflected contribution which has an amplitude given by $\mathrm{Re}\, \Gamma$ and which appears to emanate from the image point $(0, -z')$ (located in a medium with wave velocity c_1). This result assumes that both the source and observation point are situated in the optically thinner medium $(c_1 > c_2)$. If $c_1 < c_2$, an additional contribution may arise from the branch point singularity at $w_b = \sin^{-1}\sqrt{\varepsilon}$ which now lies in the range $0 < w_b < \pi/2$ (see Fig. 2; the branch point contribution yields a diffracted wave front which corresponds to the lateral wave sketched in Fig. 5.13'). Complications occur when the media are dissipative or dispersive, i.e., for complex dielectric constants $\bar{\varepsilon}(s) = \varepsilon_r + \sigma/s$, σ = conductivity, or for $\varepsilon_r = \varepsilon_r(\omega)$, in which case $\Gamma(w)$ is also a function of s. For observation points lying in medium 2 the evaluation (even for the lossless, non-dispersive case) is more difficult since the exponent of the resulting integrand (cf. Eq. (5.113)) does not have the simple form exhibited in Eq. (12a). (See Problem 2).

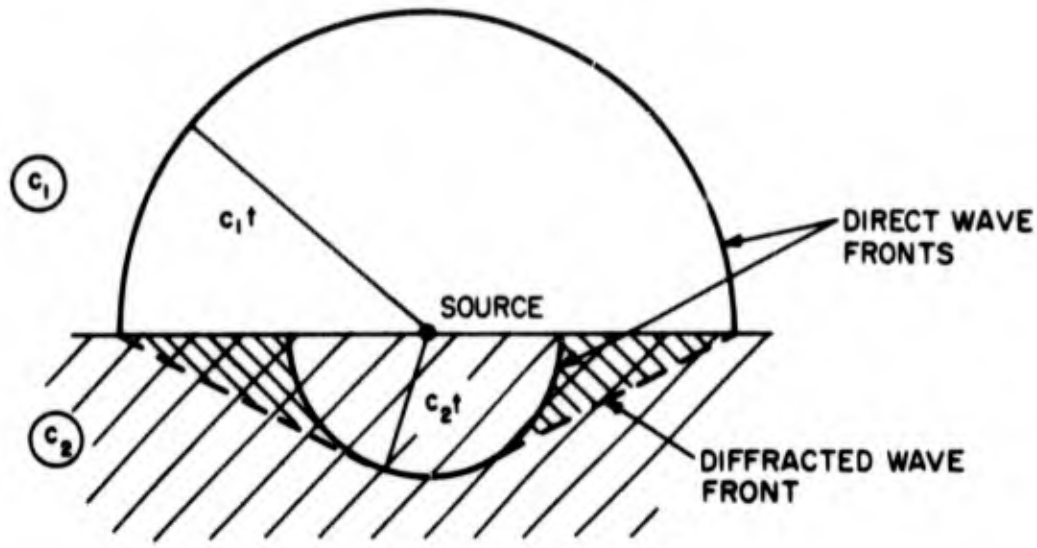

Fig. 2 - Wave fronts when source is on interface. Points in vertically shaded region are reached first by diffracted wave, along a ray path corresponding to that of lateral wave in Fig. 5.13'.

2. Point source

Consider the longitudinal dipole source in Eq. (22) located at the point $\underline{r}' = (0, 0, z')$, $z' < 0$, in front of a semi-infinite dielectric region $z > 0$ (see Fig. 5.13). The electromagnetic fields in this case are inferred via Eqs. (8) from the scalar Green's function $\hat{G}'$ which, for $z < 0$, is separable into a free-space and a reflected part. The free-space solution is given in Eqs. (25), with r representing the distance from the source point to the observation point. A cylindrical waveguide representation for the steady-state reflected wave contribution is given in Eq. (5.87). Because of the occurrence of the Hankel function in the integrand of this latter equation, it is not possible to apply Eqs. (12) - (15) directly, and the recovery of the transient response is considerably more involved than for the line source problem. It is nevertheless instructive to perform the analysis since the result for impulsive excitation may be manipulated into an explicit form requiring the integration of the reflection

coefficient. The integration proceeds between finite limits, and while it does not seem possible to reduce the integral further, numerical methods may be resorted to for specific evaluation.

It seems best to employ a procedure[3] which utilizes the rectangular waveguide representation (see Eqs. (5.18) and (5.83), for an exp(jωt) dependence):

$$G_s'(\underline{r},\underline{r}';\omega) = \frac{j}{8\pi^2}\int_{-\infty}^{\infty} d\xi \int_{-\infty}^{\infty} d\eta \; \frac{e^{-j\xi x - j\eta y - j\kappa_1 Z}}{\kappa_1}\,\Gamma(\kappa_1,\kappa_2) \quad , \tag{32}$$

where $Z = |z+z'|$ and

$$\Gamma(\kappa_1,\kappa_2) = -\frac{\varepsilon_2\kappa_1 - \varepsilon_1\kappa_2}{\varepsilon_2\kappa_1 + \varepsilon_1\kappa_2} \quad , \quad \kappa_{1,2} = \sqrt{\frac{\omega^2}{c_{1,2}^2} - \xi^2 - \eta^2} \quad , \quad \mathrm{Im}\,\kappa_{1,2} \le 0 \quad . \tag{32a}$$

Next let $\omega \to -js$, $s > 0$, and introduce the change of scale $\xi = \alpha' s$, $\eta = \beta' s$, which renders Γ independent of s and also allows the factor s to appear explicitly in the exponential:

$$\bar{G}_s'(\underline{r},\underline{r}';s) = -\frac{s}{8\pi^2}\int_{-\infty}^{\infty}\int_{-\infty}^{\infty} \frac{e^{s(-j\alpha' x - j\beta' y - \gamma_1' Z)}}{\gamma_1'}\,\Gamma(\gamma_1',\gamma_2')\,d\alpha'\,d\beta' \quad , \tag{33}$$

where

$$\gamma_{1,2}' = \sqrt{\frac{1}{c_{1,2}^2} + \alpha'^2 + \beta'^2} \quad , \quad \mathrm{Re}\,\gamma_{1,2}' \ge 0 \quad . \tag{33a}$$

Cylindrical coordinates (ρ,ϕ) in the x-y plane are now introduced via a change of variable which makes the direction of the vector $(\underline{x}_o\alpha' + \underline{y}_o\beta')$ identical to that of the radius vector $\underline{\rho} = \rho(\underline{x}_o\cos\phi + \underline{y}_o\sin\phi) = (\underline{x}_o x + \underline{y}_o y)$:

$$\alpha' = \alpha\cos\phi - \beta\sin\phi \quad , \quad \beta' = \alpha\sin\phi + \beta\cos\phi \quad . \tag{34}$$

Thus,

$$\alpha' x + \beta' y = \alpha\rho \quad , \quad \alpha'^2 + \beta'^2 = \alpha^2 + \beta^2 \quad , \quad d\alpha' d\beta' = d\alpha d\beta \quad , \tag{34a}$$

so that Eq. (33) can be written as[3]

$$\bar{G}_s'(\underline{r},\underline{r}';s) = -\frac{s}{8\pi^2}\int_{-\infty}^{\infty} d\beta \int_{-\infty}^{\infty} \frac{e^{s(-j\alpha\rho - \gamma_1 Z)}}{\gamma_1}\,\Gamma(\gamma_1,\gamma_2)\,d\alpha \quad , \tag{35}$$

where

$$\gamma_{1,2} = \sqrt{\alpha^2 + \psi_{1,2}^2} \quad , \quad \psi_{1,2} = \sqrt{\frac{1}{c_{1,2}^2} + \beta^2} \quad , \quad \mathrm{Re}\,\gamma_{1,2} \geq 0 \quad , \quad \psi_{1,2} > 0 \quad . \tag{35a}$$

The integral over α can be cast into the form (13). First, apply the transformation

$$\alpha = \psi_1 \sinh \gamma \quad , \tag{36}$$

so that $\gamma_1 = \psi_1 \cosh \gamma$. Upon also utilizing spherical coordinates $(\hat{r}, \theta)$ via $\rho = \hat{r} \sin \theta$, $Z = \hat{r} \cos \theta$, $0 < \theta < \pi/2$, one obtains

$$I = \int_{-\infty}^{\infty} \frac{e^{-s(j\alpha\rho + \gamma_1 Z)}}{\gamma_1} \Gamma(\gamma_1, \gamma_2)\, d\alpha = \int_{-\infty}^{\infty} e^{-s\hat{r}\psi_1 \cosh(\gamma + j\theta)} \Gamma(\gamma_1, \gamma_2) d\gamma \quad . \tag{37}$$

With $\gamma = -jw$,

$$I = -j \int_{-j\infty}^{j\infty} e^{-s\hat{r}\psi_1 \cos(w-\theta)} \Gamma(w) dw \quad , \quad \Gamma(w) = \frac{\varepsilon_2 \cos w - \varepsilon_1 \sqrt{\frac{\psi_2^2}{\psi_1^2} - \sin^2 w}}{\varepsilon_2 \cos w + \varepsilon_1 \sqrt{\frac{\psi_2^2}{\psi_1^2} - \sin^2 w}} \quad , \tag{38a}$$

or, equivalently,

$$I = -j \int_{-j\infty}^{j\infty} e^{-s\hat{r}\psi_1 \cos w} \Gamma(w + \theta)\, dw \quad . \tag{38b}$$

The transition from (38a) to (38b) is permitted if Γ has no singularities in the strip $0 < |\mathrm{Re}\, w| < \pi/2$. If $\psi_1 < \psi_2$, i.e., $\varepsilon_2 > \varepsilon_1$, the branch point singularities w_b lie on the lines $\mathrm{Re}\, w = \pm\pi/2$. The pole singularities w_p of Γ are located at

$$\cos w_p = -\sqrt{\frac{\left(\frac{\psi_2}{\psi_1}\right)^2 - 1}{\varepsilon - 1}} \quad , \quad \varepsilon = \frac{\varepsilon_2}{\varepsilon_1} = \frac{c_1^2}{c_2^2} \quad . \tag{39}$$

$\cos w_p$ is real when $\epsilon > 1$, and must be chosen negative since $\sqrt{(\psi_2/\psi_1)^2 - \sin^2 w} > 0$ when the radicand is positive. Hence, the poles also lie outside the range $|\mathrm{Re}\, w| < \pi/2$, and Eq. (38b) is valid for $0 < \theta < \pi/2$ when $\epsilon > 1$. Thus, from Eq. (14),

$$I = 2 \int_{\hat{r}\psi_1}^{\infty} \frac{e^{-s\tau}}{\sqrt{\tau^2 - (\hat{r}\psi_1)^2}} \mathrm{Re}\, \Gamma\left[\theta + j \cosh^{-1}\left(\frac{\tau}{\hat{r}\psi_1}\right)\right] d\tau \quad , \quad \epsilon > 1 \quad , \tag{40}$$

with ψ_1 defined in Eq. (35a).

The desired formulation in Eq. (9a) is achieved after substituting Eq. (40) into (35) and interchanging the orders of integration.[3] The τ-integration extends from the curve $\tau = \hat{r}\sqrt{(1/c_1)^2 + \beta^2}$ to $\tau = \infty$, while $-\infty < \beta < \infty$. If the β-integration is performed first, one has $\left[(\tau/\hat{r})^2 - 1/c_1^2\right] < |\beta|$, while $(\hat{r}/c_1) < \tau < \infty$. Thus,

$$\bar{G}'_s(\underline{r}, \underline{r}'; s) = -\frac{s}{4\pi^2} \int_0^{\infty} e^{-s\tau} A(\tau) d\tau \quad , \tag{41}$$

where

$$A(\tau) = \begin{cases} 0 \quad , & \tau < \dfrac{\hat{r}}{c_1} \quad , \qquad (41a) \\[2ex] \displaystyle\int_{-\psi}^{\psi} \frac{\mathrm{Re}\, \Gamma\left[\theta + j \cosh^{-1}\left(\frac{\tau}{\hat{r}\psi_1}\right)\right]}{\sqrt{\tau^2 - (\hat{r}\psi_1)^2}} d\beta \quad , & \tau > \dfrac{\hat{r}}{c_1} \quad , \qquad (41b) \end{cases}$$

and $\psi = \left[(\tau/\hat{r})^2 - 1/c_1^2\right]^{1/2}$, $\psi_1^2 = (1/c_1^2) + \beta^2$. A final change of variable

$$\beta = \left[\left(\frac{\tau}{\hat{r}}\right)^2 - \frac{1}{c_1^2}\right]^{1/2} \sin \alpha \tag{42}$$

transforms Eq. (41b) into

$$A(\tau) = \frac{2}{\hat{r}} \int_0^{\pi/2} \mathrm{Re}\, \Gamma\left[\theta + j \cosh^{-1} \frac{\tau}{\sqrt{\tau^2 + (\hat{r}/c_1)^2 \cos^2 \alpha}}\right] d\alpha \quad . \tag{43}$$

Hence, the temporal Green's function $\hat{G}'$ is obtained from Eq. (11) as

$$\hat{G}'_s(\underline{r}, \underline{r}';t) = \begin{cases} -\dfrac{1}{4\pi^2} \displaystyle\int_{\hat{r}/c_1}^{t} \dfrac{d\hat{q}(t-\alpha)}{dt} A(\alpha)\, d\alpha \quad , & t > \dfrac{\hat{r}}{c_1} \quad , \\ 0 \quad , & t < \dfrac{\hat{r}}{c_1} \quad , \end{cases} \tag{44a, 44b}$$

which, for excitation by a unit step function $\hat{q}(t) = 1$ when $t > 0$, $\hat{q}(t) = 0$ when $t < 0$, reduces in view of $d\hat{q}/dt = \delta(t)$ to[3, 4]

$$\hat{G}'_s(\underline{r}, \underline{r}';t) = \begin{cases} \dfrac{1}{4\pi^2} A(t) \quad , & t > \dfrac{\hat{r}}{c_1} \\ 0 \quad , & t < \dfrac{\hat{r}}{c_1} \quad . \end{cases} \tag{45}$$

This expression for the potential function and the associated fields is considerably more complicated than that in Eq. (31) pertaining to the line source excitation. When the source and observation points are both situated on the interface, the result can be expressed in terms of elementary functions.[5] This reduction is left as an exercise for the reader.

D. Pulsed Sources in the Presence of a Wedge

The problems in this section illustrate how the transient field is influenced by the presence of edge singularities on the surface of a scatterer. This effect is demonstrated in its simplest form by a perfectly absorbing wedge which, in the high-frequency time-harmonic analysis, gives rise to a diffraction field only, without a reflected contribution (see Sec. 6D). Since the exact integral formulas for the time-harmonic case have (or are readily cast into) the form given in Eqs. (12), the transient solution is obtained and interpreted with ease. After the incident wave front strikes the edge, a diffracted wave front emerges radially from the edge. It is found that diffraction weakens the field singularities across the wave front (see for example Eq. (59)); i. e., the singularities are less strong across the diffracted front than across the incident front. This behavior may be understood if it is recalled that in the time-harmonic high-frequency limit, diffraction effects diminish more rapidly with k than those represented by the geometric-optical (in particular, the incident) field. Consequently, Eq. (6b) predicts a less violent behavior for the diffraction field. Analogous conclusions are valid for the perfectly conducting wedge which generates reflected fields, in addition.

The excitation of a "perfectly absorbing" and a perfectly conducting wedge by various time-harmonic sources has been considered in Sec. 6. D. For simplicity, we consider only longitudinally directed sources whence the evaluation of the electromagnetic fields is reduced via Eqs. (8) to that of determining the scalar Green's functions $\hat{G}'$ and $\hat{G}''$. However, from the remarks in Sec. A, these considerations can also be applied to arbitrarily directed sources which then require the determination of the functions $\hat{S}'(\underline{r}, t)$ and $\hat{S}''(\underline{r}, t)$ in Sec. 2.9.

1. Absorbing wedge

a. Line source excitation

A line source of electric or magnetic current is situated at $\underline{\rho}' = (\rho', \phi')$ in the presence of a wedge, as shown in Fig. 6.5.* If the wedge faces are "perfectly absorbing" in the sense discussed in Sec. 6. D1, $\hat{G}'$ and $\hat{G}''$ are identical and equal to the infinite angular space Green's function $\hat{G}_\infty$. Suitable for our purpose is the representation (6. 34) of the steady-state Green's function $G_\infty(\underline{\rho}, \underline{\rho}'; \omega)$ ($\exp(-i\omega t)$ dependence):

---

*Fig. 5 of Chapter VI.

$$G_\infty(\underline{\rho}, \underline{\rho}';\omega) = \frac{i}{4} H_o^{(1)}(k|\underline{\rho}-\underline{\rho}'|)\, \eta(\pi - |\phi-\phi'|)$$

$$- \frac{1}{8\pi} \int_{-i\infty}^{i\infty} H_o^{(1)}\left(k \sqrt{\rho^2 + \rho'^2 + 2\rho\rho' \cos w}\right) \check{A}(\phi, \phi';w)\,dw \quad , \tag{46}$$

where

$$\check{A}(\phi, \phi';w) = \frac{1}{\pi - |\phi-\phi'| - w} + \frac{1}{\pi + |\phi-\phi'| + w} \quad , \tag{47}$$

and $\eta(x) = 1$ or 0 when $x > 0$ or $x < 0$, respectively. Upon letting $k \to is/c$, where s is positive and c is the speed of light in the exterior medium, and recalling that

$$H_\nu^{(1)}(iz) = \frac{2}{\pi i} e^{-i\nu\pi/2} K_\nu(z) \quad , \tag{48}$$

one obtains

$$\bar{G}_\infty(\underline{\rho}, \underline{\rho}';s) = \frac{1}{2\pi} K_o\left(s \frac{|\underline{\rho}-\underline{\rho}'|}{c}\right) \eta(\pi - |\phi-\phi'|) + \bar{I}(\underline{\rho}, \underline{\rho}';s) \quad , \tag{49}$$

with

$$\bar{I}(\underline{\rho}, \underline{\rho}';s) = \frac{i}{4\pi^2} \int_{-i\infty}^{i\infty} K_o\left(\frac{s}{c} \sqrt{\rho^2 + \rho'^2 + 2\rho\rho' \cos w}\right) \check{A}(\phi, \phi';w)\,dw \quad . \tag{50}$$

The inversion of the first term on the right-hand side of Eq. (49) is given in Eq. (20). To transform the second term into a representation as in Eq. (9a), introduce

$$K_o(x) = \int_1^\infty \frac{e^{-xt}}{\sqrt{t^2-1}}\, dt \quad , \qquad x > 0 \quad , \tag{51}$$

to obtain

$$\bar{I}(\underline{\rho}, \underline{\rho}';s) = \frac{i}{4\pi^2} \int_{-i\infty}^{i\infty} dw\, \check{A}(\phi, \phi';w) \int_{\frac{f}{c}}^\infty \frac{e^{-s\tau}}{\sqrt{\tau^2 - \frac{f^2}{c^2}}}\, d\tau \quad , \tag{52}$$

where

$$f \equiv f(\beta) = \sqrt{\rho^2 + \rho'^2 + 2\rho\rho' \cosh\beta} > 0 \quad , \qquad \beta = -iw \quad . \tag{52a}$$

The desired formulation results upon interchanging the orders of integration which, in Eq. (52), cover the range $f(\beta) < c\tau < \infty$ and $-\infty < \beta < \infty$. If the β-integration is performed first, one has $-\psi(\tau) < \beta < \psi(\tau)$, $\psi(\tau) = \cosh^{-1}\left[\left(c^2\tau^2 - \rho^2 - \rho'^2\right)/2\rho\rho'\right]$, while $f(0) < c\tau < \infty$. Thus

$$\bar{\Gamma}(\underline{\rho}, \underline{\rho}'; s) = \int_0^\infty e^{-s\tau} A(\tau)\, d\tau \tag{53}$$

where

$$A(\tau) = \begin{cases} 0 \quad , & c\tau < (\rho + \rho') \quad , \qquad (54a) \\ -\dfrac{1}{4\pi^2} \displaystyle\int_{-\psi(\tau)}^{\psi(\tau)} \dfrac{\check{A}(\phi, \phi'; i\beta)}{\sqrt{\tau^2 - \dfrac{f^2(\beta)}{c^2}}}\, d\beta \quad , & c\tau > (\rho + \rho') \quad . \qquad (54b) \end{cases}$$

If the temporal variation of the line source is given by $\hat{q}(t)$, with $\hat{q}(t) = 0$ when $t < 0$, one obtains from Eqs. (11), (20), (51) and (54),

$$\hat{G}_\infty(\underline{\rho}, \underline{\rho}'; t) = \frac{1}{2\pi}\eta(\pi - |\phi - \phi'|)\,\eta\left(t - \frac{|\underline{\rho} - \underline{\rho}'|}{c}\right) \int_{\frac{|\underline{\rho} - \underline{\rho}'|}{c}}^{t} \hat{q}(t-a) \frac{1}{\sqrt{a^2 - \dfrac{|\underline{\rho} - \underline{\rho}'|^2}{c^2}}}\, da$$

$$+ \eta\left(t - \frac{(\rho + \rho')}{c}\right) \int_{\frac{(\rho+\rho')}{c}}^{t} \hat{q}(t-a)\, A(a)\, da \quad , \tag{55}$$

where

$$A(a) = -\frac{1}{2\pi^2} \int_0^{\cosh^{-1} M} \frac{\mathrm{Re}\, \check{A}(\phi, \phi'; i\beta)}{\sqrt{a^2 - \dfrac{f^2(\beta)}{c^2}}}\, d\beta \quad , \tag{55a}$$

$$M = \frac{c^2 a^2 - \rho^2 - \rho'^2}{2\rho\rho'} \quad . \tag{55b}$$

The first term on the right-hand side of Eq. (55) represents the response in the absence of the wedge and exists only outside the shadow region of Fig. 6.5. The second term represents a cylindrically spreading diffracted pulse which exists in the entire region exterior to the wedge and reaches the observation point $P(\rho, \phi)$ at time $t = (\rho+\rho')/c$, i. e., after a time interval required to travel both the distance ρ' from the source point to the edge and the distance ρ from the edge to the observation point. In view of the "absorbing" wedge faces there is no reflected pulse contribution. The incident and diffracted wave fronts are sketched in Fig. 3.

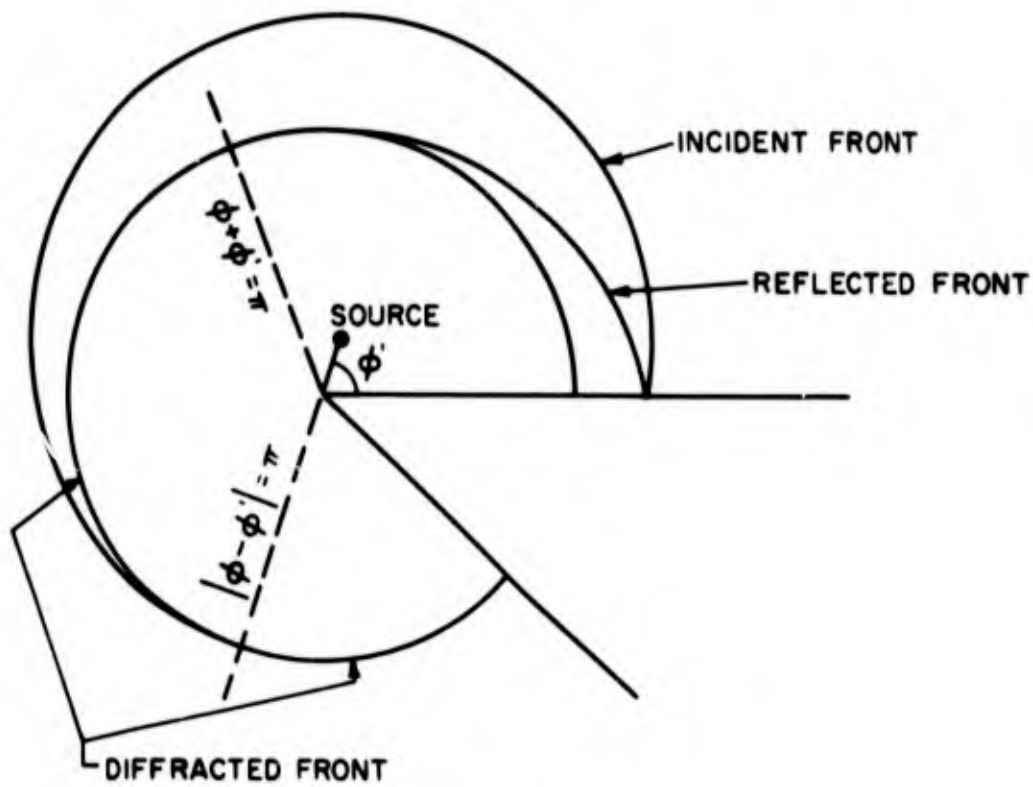

Fig. 3 - Diffraction of cylindrical pulse by a wedge (omit reflected front for perfectly absorbing case) The incident front is centered at the source, the reflected front at the source image with respect to the horizontal wedge face, and the diffracted front is centered at the edge.

b. Plane wave excitation

If the source point ρ' moves to infinity along the direction ϕ', one employs instead of Eq. (46) the appropriate plane wave formulation (see Eq. 6.37) wherein one replaces

$$\frac{i}{4} H_0^{(1)}\left(k\sqrt{\rho^2 + \rho'^2 + 2\rho\rho' \cos a}\right) \qquad \text{by} \qquad e^{ik\rho \cos a} \quad .$$

Hence, one has instead of Eq. (49),

$$\bar{G}_\infty(\underline{\rho}, \phi'; s) = e^{s\frac{\rho}{c}\cos(\phi-\phi')} \eta(\pi - |\phi-\phi'|) + \bar{I}(\underline{\rho}, \phi'; s) \quad , \tag{56}$$

$$\bar{I}(\underline{\rho}, \phi'; s) = \frac{i}{2\pi} \int_{-i\infty}^{i\infty} e^{-(s\rho \cos w)/c} \check{A}(\phi, \phi'; w) dw \quad , \tag{56a}$$

which is directly in the form (13). Thus, from Eqs. (14),

$$\bar{G}_\infty(\underline{\rho}, \phi'; s) = \eta(\pi - |\phi-\phi'|) \int_0^\infty e^{-s\tau} \delta\left(\tau + \frac{\rho}{c}\cos(\phi-\phi')\right) d\tau - \frac{1}{\pi} \int_{\rho/c}^\infty d\tau\, e^{-s\tau} \frac{\mathrm{Re}\, \check{A}(\phi, \phi'; i\beta)}{\sqrt{\tau^2 - \left(\frac{\rho}{c}\right)^2}} \quad , \tag{57}$$

and for a source variation $\hat{q}(t)$ when $t > 0$,

$$\hat{G}_\infty(\underline{\rho}, \phi'; t) = \hat{q}\left(t + \frac{\rho}{c}\cos(\phi-\phi')\right) \eta(\pi - |\phi-\phi'|) - \frac{1}{\pi} \eta\left(t - \frac{\rho}{c}\right) \int_{\rho/c}^t \hat{q}(t-a) \frac{\mathrm{Re}\, \check{A}(\phi, \phi'; i\beta)}{\sqrt{a^2 - \left(\frac{\rho}{c}\right)^2}} da \quad , \tag{58}$$

where $\beta = \cosh^{-1}(a\, c/\rho)$.

For an impulsive excitation $\hat{q}(t) = \delta(t-t')$, Eq. (58) becomes

$$\hat{G}_\infty(\underline{\rho}, \phi'; t) = \delta\left(t-t' + \frac{\rho}{c}\cos(\phi-\phi')\right)\eta(\pi - |\phi-\phi'|) - \frac{1}{\pi} \frac{\mathrm{Re}\, \check{A}\left[\phi, \phi'; i \cosh^{-1}(c(t-t')/\rho)\right]}{\sqrt{(t-t')^2 - \left(\frac{\rho}{c}\right)^2}} \eta\left(t-t' - \frac{\rho}{c}\right) , \tag{59}$$

which is simpler than the corresponding line source result since no integration as in Eq. (55a) is required. This result again highlights the cylindrical wave character of the diffracted wave propagating outward from the edge, as shown in Fig. 4 for $t' = 0$ (see also Fig. 6.6).

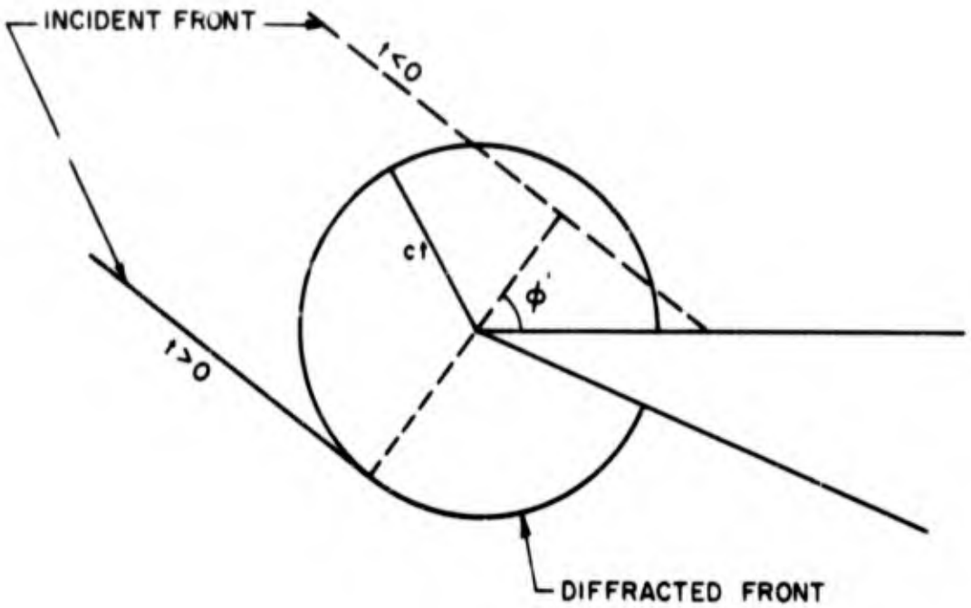

Fig. 4 - Diffraction of plane wave pulse by perfectly absorbing wedge (no diffracted pulse when $t < 0$)

c. Point source excitation

For point source excitation at $\underline{r}' = (\rho', \phi', z')$, the steady-state Green's function $G_\infty(\underline{r}, \underline{r}'; \omega)$ is given as in Eq. (46), provided one replaces (cf. Eq. 6.42)

$$\frac{i}{4} H_0^{(1)}\left(k\sqrt{\rho^2 + \rho'^2 + 2\rho\rho' \cos\alpha}\right) \text{ by } \frac{e^{ik\zeta}}{4\pi\zeta} \quad , \quad \zeta = \sqrt{\rho^2 + \rho'^2 + 2\rho\rho' \cos\alpha + (z-z')^2} \ .$$

The resulting expression for $\bar{G}_\infty(\underline{r}, \underline{r}'; s)$ is similar to Eq. (56) except that $\rho \cos\alpha$ is replaced by ζ and a factor $(1/4\pi\zeta)$ is added. Proceeding as in Eq. (13), with $\tau = (\zeta/c)$, one may derive an integral formulation similar in form to that in Eq. (14), and one finds for the time function corresponding to the impulse excitation $\hat{q}(t) = \delta(t-t')$:

$$\hat{G}_\infty(\underline{r}, \underline{r}'; t) = \frac{\delta\left(t-t' - \frac{|\underline{r}-\underline{r}'|}{c}\right)}{4\pi|\underline{r}-\underline{r}'|} \eta(\pi - |\phi-\phi'|) + \frac{c}{4\pi} \frac{\mathrm{Re}\, \check{A}(\phi, \phi'; i\beta)}{\rho\rho' \sinh\beta} \eta\left(t-t' - \frac{\bar{R}}{c}\right) \quad , \qquad (60)$$

where $\beta = \cosh^{-1}\left[\left(c^2(t-t')^2 - \rho^2 - \rho'^2 - (z-z')^2\right)/2\rho\rho'\right]$ and $\bar{R} = \left[(\rho+\rho')^2 + (z-z')^2\right]^{1/2}$. In this instance, the diffracted wave front reaches the observation point along a ray path ℓ_1 which strikes the edge and is reflected therefrom along ℓ_2 at the incidence angle. The diffracted rays, perpendicular to the wave front, lie on a cone as shown in Fig. 6.9.

2. Perfectly conducting wedge and half plane

If the wedge is perfectly conducting, the vanishing of the tangential component of the electric field at the wedge surface is assured through use of the E mode Green's function $\hat{G}'$ and the H mode Green's function $\hat{G}''$, both of which can be constructed as a superposition of an infinite set of "perfectly absorbing" wedge solutions $\hat{G}_\infty$. Details concerning this image representation of the time-harmonic Green's functions $G'(\underline{r}, \underline{r}';\omega)$ and $G''(\underline{r}, \underline{r}';\omega)$ have been given in Sec. 6.D3. Inspection of these solutions reveals that the Green's functions for the perfectly conducting wedge differ from those for the perfectly absorbing wedge only through the presence of additional geometrically reflected contributions and through the appearance of a different function in the integrand of the integral representation for the diffracted field. Consequently, the recovery of the transient response for the perfectly conducting wedge is carried out at once in terms of the solutions obtained in the preceding section. For simplicity, it will be assumed that the exterior wedge angle ϖ is greater than π; for $\varpi < \pi$, the functional form of the solution is unaltered save for the inclusion of additional geometrically reflected wave contributions which may arise as a result of multiple reflections between the wedge faces.

a. Line source excitation

The time-harmonic Green's functions G' and G'', given in Eqs. (6.94), are (for an $\exp(-i\omega t)$ time dependence):

$$\left.\begin{matrix} G'(\underline{\rho}, \underline{\rho}';\omega) \\ G''(\underline{\rho}, \underline{\rho}';\omega) \end{matrix}\right\} = \frac{i}{4} H_o^{(1)}\left[kR(\phi-\phi')\right] \eta\left[\pi - |\phi-\phi'|\right]$$
$$\mp \frac{i}{4} H_o^{(1)}\left[kR(\phi+\phi')\right] \eta\left[\pi - (\phi+\phi')\right]$$
$$\mp \frac{i}{4} H_o^{(1)}\left[kR(2\varpi-\phi-\phi')\right] \eta\left[\pi - (2\varpi-\phi-\phi')\right]$$
$$- \frac{1}{8\pi} \int_{-i\infty}^{i\infty} H_o^{(1)}\left[kR(w-\pi)\right] \left[B(\phi, \phi';w) \mp B(\phi, -\phi';w)\right] dw, \quad \varpi > \pi \quad , \tag{61}$$

where

$$R(a) = (\rho^2 + \rho'^2 - 2\rho\rho' \cos a)^{1/2} \quad , \tag{61a}$$

and

$$B(\phi, \phi'; w) = \frac{\pi}{\varphi} \frac{\sin \frac{\pi}{\varphi}(w-\pi)}{\cos \frac{\pi}{\varphi}(w-\pi) - \cos \frac{\pi}{\varphi}(\phi-\phi')} \quad . \tag{61b}$$

The first three terms on the right-hand side of Eq. (61) represent the incident field and the fields reflected from the wedge faces at $\phi = 0$ and $\phi = \varphi$, respectively; if $\varphi < \pi$, the solution includes additional reflected wave (image) contributions but is otherwise unchanged. Comparison of Eqs. (61) and (46) reveals their identical form if A in the integrand of Eq. (46) is replaced by $\left[B(\phi, \phi'; w) \mp B(\phi, -\phi'; w)\right]$. The transient solution corresponding to a temporal source function $\hat{f}(t)$ when $t > 0$ is therefore given via Eq. (55) by

$$\left.\begin{matrix}\hat{G}'(\underline{\rho}, \underline{\rho}'; t) \\ \hat{G}''(\underline{\rho}, \underline{\rho}'; t)\end{matrix}\right\} = \frac{c}{2\pi} \eta\left[\pi - |\phi-\phi'|\right] \eta\left[t - \frac{R(\phi-\phi')}{c}\right] \int_{R(\phi-\phi')/c}^{t} \frac{\hat{f}(t-a)da}{\sqrt{(ac)^2 - R^2(\phi-\phi')}}$$

$$\mp \frac{c}{2\pi} \eta\left[\pi - (\phi+\phi')\right] \eta\left[t - \frac{R(\phi+\phi')}{c}\right] \int_{R(\phi+\phi')/c}^{t} \frac{\hat{f}(t-a)da}{\sqrt{(ac)^2 - R^2(\phi+\phi')}}$$

$$\mp \frac{c}{2\pi} \eta\left[\pi - (2\varphi - \phi-\phi')\right] \eta\left[t - \frac{R(2\varphi - \phi-\phi')}{c}\right] \int_{R(2a-\phi-\phi')/c}^{t} \frac{\hat{f}(t-a)\, da}{\sqrt{(ac)^2 - R^2(2a-\phi-\phi')}}$$

$$+ \eta\left[t - \frac{(\rho+\rho')}{c}\right] \int_{(\rho+\rho')/c}^{t} \hat{f}(t-a)\left[D(\phi, \phi'; a) \mp D(\phi, -\phi'; a)\right] da \quad , \tag{62}$$

where

$$D(\phi, \phi'; a) = -\frac{c}{2\pi^2} \int_0^{\cosh^{-1} M} \frac{d\beta}{\sqrt{(ac)^2 - f^2(\beta)}} \operatorname{Re} B(\phi, \phi'; i\beta) \tag{62a}$$

$$M = \frac{c^2 a^2 - \rho^2 - \rho'^2}{2\rho\rho'} \quad . \tag{62b}$$

One verifies from Eq. (61b) that

$$\mathrm{Re}\, B(\phi, \phi'; i\beta) = \frac{\pi}{\varphi} \frac{\left(\cos\frac{\pi\psi}{\varphi}\cosh\frac{\pi\beta}{\varphi} - \cos\frac{\pi^2}{\varphi}\right)\sin\frac{\pi^2}{\varphi}}{\cosh^2\frac{\pi\beta}{\varphi} + \cos^2\frac{\pi\psi}{\varphi} - \sin^2\frac{\pi^2}{\varphi} - 2\cos^2\frac{\pi^2}{\varphi}\cos\frac{\pi\psi}{\varphi}\cosh\frac{\pi\beta}{\varphi}}, \quad \psi = (\phi - \phi'). \tag{63}$$

$f(\beta)$ is defined in Eq. (52a). The physical interpretation of this result is as sketched in Fig. 3.

While it does not seem possible to evaluate D in closed form when φ is arbitrary, the integral can be reduced for the special case of a half-plane $\varphi = 2\pi$,[6,7] in which instance,

$$\mathrm{Re}\, B(\phi, \phi'; i\beta) = \frac{\cos\frac{\psi}{2}\cosh\frac{\beta}{2}}{\cosh\beta + \cos\psi}, \qquad \varphi = 2\pi. \tag{64}$$

Introduction of the successive changes of variable

$$\cosh\beta = 1 + v^2, \qquad \cosh\frac{\beta}{2}\, d\beta = \sqrt{2}\, dv, \tag{65a}$$

and

$$v = b\sin\gamma, \qquad b = \sqrt{\frac{(ca)^2 - (\rho+\rho')^2}{2\rho\rho'}}, \tag{65b}$$

reduces Eq. (62a) to

$$D(\phi, \phi'; a) = -\frac{c}{2\pi^2}\frac{\cos\frac{\psi}{2}}{\sqrt{\rho\rho'}}\int_0^{\pi/2}\frac{d\gamma}{1 + \cos\psi + b^2\sin^2\gamma}, \tag{66}$$

which can be evaluated to yield

$$D(\phi, \phi'; a) = -\frac{\cos\frac{\psi}{2}}{\sqrt{\rho\rho'}}\frac{c}{4\pi}\frac{1}{\sqrt{2\cos^2\frac{\psi}{2}}\sqrt{1 + \cos\psi + b^2}} = -\frac{c}{4\pi\sqrt{(ca)^2 - R^2(\psi)}}\,\mathrm{sgn}\cos\frac{\psi}{2}, \tag{67}$$

where $\mathrm{sgn}\, x = \pm 1$, $x \gtrless 0$, and $R(\psi)$ is defined in Eq. (61a). Hence, for an impulsive source distribution $\hat{f}(t) = \delta(t - t')$, $t' > 0$, one obtains for the half-plane Green's functions,

$$\left.\begin{matrix}\hat{G}'(\underline{\rho},\underline{\rho}';t)\\ \hat{G}''(\underline{\rho},\underline{\rho}';t)\end{matrix}\right\} = \frac{c}{2\pi}\,\eta\left[\pi - |\phi-\phi'|\right]\eta\left[\hat{t} - \frac{R(\phi-\phi')}{c}\right]\frac{1}{\sqrt{(c\hat{t})^2 - R^2(\phi-\phi')}}$$

$$\mp \frac{c}{2\pi}\,\eta\left[\pi - (\phi+\phi')\right]\eta\left[\hat{t} - \frac{R(\phi+\phi')}{c}\right]\frac{1}{\sqrt{(c\hat{t})^2 - R^2(\phi+\phi')}}$$

$$- \frac{c}{4\pi}\,\eta\left[\hat{t} - \frac{(\rho+\rho')}{c}\right]\left[\frac{\mathrm{sgn}(\pi - |\phi-\phi'|)}{\sqrt{(c\hat{t})^2 - R^2(\phi-\phi')}} \mp \frac{\mathrm{sgn}(\pi - \phi - \phi')}{\sqrt{(c\hat{t})^2 - R^2(\phi+\phi')}}\right] \quad , \qquad (68)$$

with $\hat{t} = t - t'$. In view of the symmetry of the half-plane configuration, it has been assumed without loss of generality that $\phi' < \pi$. The various geometric-optical regions entering into Eq. (68) are illustrated in Figs. 3 and 6.11. The simple result in Eq. (68) demonstrates again that diffraction weakens the singularity which exists across the incident wave front; the diffracted field is in fact finite, except along the geometric-optical boundary lines. (The reader may find it instructive to deduce the field behavior near the wave fronts from the time-harmonic asymptotic solution in Eq. (6.103) in conjunction with Eqs. (6)).

b. Plane wave or point source excitation

The preceding considerations also lead directly to the transient solutions for plane wave or point source excitation. For an impulsive source distribution $\hat{f}(t) = \delta(t-t')$, one has for a plane wave incident on a wedge with exterior angle $\varphi > \pi$,

$$\left.\begin{matrix}\hat{G}'(\underline{\rho},\underline{\rho}';t)\\ \hat{G}''(\underline{\rho},\underline{\rho}';t)\end{matrix}\right\} = \delta\left[\hat{t} + \frac{\rho}{c}\cos(\phi-\phi')\right]\eta\left[\pi - |\phi-\phi'|\right] \mp \delta\left[\hat{t} + \frac{\rho}{c}\cos(\phi+\phi')\right]\eta\left[\pi - (\phi+\phi')\right]$$

$$\mp \delta\left[\hat{t} + \frac{\rho}{c}\cos(2\varphi - \phi - \phi')\right]$$

$$- \frac{c}{\pi}\,\frac{\eta\left(\hat{t} - \frac{\rho}{c}\right)}{\sqrt{(c\hat{t})^2 - \rho^2}}\left[\mathrm{Re}\,B(\phi,\phi';i\beta) \mp \mathrm{Re}\,B(\phi,-\phi';i\beta)\right] \quad , \qquad (69)$$

where $\beta = \cosh^{-1}(c\hat{t}/\rho)$.

Similarly, for an impulsive point source, one obtains an expression analogous to Eq. (60b) provided that $A(\phi,\phi';i\beta)$ is replaced by $\left[B(\phi,\phi';i\beta) \mp B(\phi,-\phi';i\beta)\right]$, and that additional reflected wave contributions are included.

E. Pulsed Line Source in the Presence of a Unidirectionally Conducting Infinite and Semi-Infinite Screen

As noted in Sec. 5.I, radiation and diffraction problems involving a unidirectionally conducting screen are of special interest since such structures may support surface waves which propagate undamped along, and decay exponentially on either side away from, the surface. These remarks apply to time-harmonic excitation, and it is of interest to explore what role is played by these wave constituents under transient conditions. Two excitation mechanisms have been considered in the time-harmonic study: a) excitation by a confined source, and b) excitation by an edge discontinuity (half plane problem). While their amplitudes depend on the mechanism involved, the surface waves in either case have identical characteristics. This behavior is altered drastically under transient conditions, and the excitation mechanism is found to be of major importance in determining the nature of the surface waves. Moreover, the presence of transient surface waves manifests itself in quite a different manner than that of their time-harmonic counterpart.

These aspects, and others pertaining to the reflected, transmitted and diffracted fields may be explored in detail from the transient solutions for a unidirectionally conducting infinite and semi-infinite screen. The results are obtained almost immediately since the time-harmonic representation integrals already have the form given in Eq. (12).[2]

1. Infinite screen

The electromagnetic properties of a unidirectionally conducting screen have been described in Sec. 5.I, and solutions have been obtained for the excitation of this structure by a time-harmonic phased line source and a dipole of electric current oriented arbitrarily in a plane parallel to the surface. While the transient solution is derived only for the case of a line current of constant strength (i.e., $\xi = 0$ in Sec. 5.I3), the procedure here may be applied as well to the evaluation of the spherical impulse response (point source excitation). If the line source is located at $y = 0$, $z = z' < 0$, and the screen occupies the $z = 0$ plane with the direction of conductivity inclined at the angle α with the x-axis, then the secondary electromagnetic fields may be derived from the scalar function (see Eq. (5.317) or (5.300a) with $\eta = k \sin w$;

a normalization factor has been included to make $(G_o + G_1)$ proportional to E_x)

$$G_1(\underline{\rho}, \underline{\rho}';\omega) = \frac{+j \cot^2 a}{4\pi} \int_{\hat{P}} \frac{e^{-jk R \cos(w-\theta)}}{\csc^2 a - \sin^2 w} dw \quad , \qquad \underline{\rho} = (y, z) \quad , \qquad (70)$$

where $y = R \sin\theta$, $|z| + |z'| = R \cos\theta$, $0 \leq \theta \leq \pi/2$, and the suppressed time dependence is $\exp(j\omega t)$. The integration path is indented into the region $|\mathrm{Re}\, w| < \pi/2$ to avoid the poles at $\sin w_p = \pm \csc a$. While the simple boundary condition in Eq. (5.271) is frequently independent, its physical realizability by a grid of thin, tightly packed wires becomes increasingly difficult when ω is very large. Since the spectrum of an impulsive source contains all frequencies, the impulse response in the presence of a physically constructed surface is not adequately described by the analysis below wherein the idealized, non-dispersive surface condition is taken to apply over the entire interval $0 < \omega < \infty$. However, if the impulse solution is utilized subsequently to synthesize the fields of a transient source with a confined frequency spectrum, the results will retain their approximate validity.

The integral representation in Eq. (70) is in the form in Eq. (12a) so that the response to a cylindrical pulse $\delta(t)$ is recovered at once from Eq. (15):

$$\hat{G}_1(\underline{\rho}, \underline{\rho}';t) = \begin{cases} 0 & , \quad t < \frac{R}{c} \quad , \quad (71a) \\ -\frac{\cos^2 a}{2\pi} \dfrac{\mathrm{Re}\left\{ \dfrac{1}{1 - \sin^2 a \, \sin^2\left[\theta + j \cosh^{-1}\left(\frac{ct}{R}\right)\right]} \right\}}{\sqrt{t^2 - \frac{R^2}{c^2}}} & , \quad t > \frac{R}{c} \quad . \quad (71b) \end{cases}$$

Thus, the transient solution contains no explicit evidence of the surface waves which play such an important role in the time-harmonic problem. The surface waves do, however, influence the transient response as shown by the investigation below. Before proceeding further, we exhibit the explicit form of the numerator term in Eq. (71b),

$$\mathrm{Re}\left\{ \quad \right\} = \frac{\csc^2 a - \cos^2\theta + \cos 2\theta (ct/R)^2}{\left[\csc^2 a - \cos^2\theta + \cos 2\theta (ct/R)^2\right]^2 + (\sin^2 2\theta)(ct/R)^2 \left[(ct/R)^2 - 1\right]} \csc^2 a \quad , \qquad (71c)$$

whence the detailed space-time behavior of the secondary field is not excessively complicated. To this contribution must be added the incident field,

$$\hat{G}_o(\underline{\rho}, \underline{\rho}';t) = \begin{cases} 0 \quad , & t < \dfrac{|\underline{\rho}-\underline{\rho}'|}{c} \quad , \qquad (72a) \\[2ex] \dfrac{1}{2\pi} \dfrac{1}{\sqrt{t^2 - \dfrac{|\rho-\rho'|^2}{c^2}}} \quad , & t > \dfrac{|\underline{\rho}-\underline{\rho}'|}{c} \quad . \qquad (72b) \end{cases}$$

One observes from Eq. (71b) that the first secondary arrival is at $t = R/c$, the time required for the pulse to travel via a geometric-optical path from the source to the screen and from the screen to the observation point. For $t \approx R/c$, the numerator in Eq. (71b) introduces little distortion so that the initial reflected field is essentially that of a simple line source at $R = 0$, modified by the angle-dependent reflection factor $-\cot^2\alpha\left[\csc^2\alpha - \sin^2\theta\right]^{-1}$. It is noted, incidentally, that the secondary potential $\hat{G}_1$ reduces to 0 when $\alpha = \pi/2$ and to $-\hat{G}_o(\underline{\rho}, \hat{\underline{\rho}}';t)$ when $\alpha = 0$, where $\hat{\underline{\rho}}'$ is the coordinate of the point $R = 0$. This behavior describes correctly the limiting cases where the screen is, respectively, perfectly transparent and perfectly reflecting.

It is worthwhile to consider two special cases for which substantial simplification occurs in Eq. (71c): $\theta = 0$ (observation points in the plane perpendicular to the screen and containing the source), and $\theta = \pi/2$ (source and observation points on the screen). In the first instance, for $t > R/c$,

$$\hat{G}_1(\underline{\rho}, \underline{\rho}';t) = -\frac{1}{2\pi} \frac{1}{\left[1 + (\tan^2\alpha)\left(\frac{ct}{R}\right)^2\right]\sqrt{t^2 - \left(\frac{R}{c}\right)^2}} \quad , \qquad \theta = 0 \quad , \qquad (73)$$

so that the reflected potential has a monotonic time behavior which is not unlike that for a perfect conductor but is accentuated by the presence of the unidirectional conductivity on the screen. The situation is quite different in the second case where one may conveniently combine the incident and secondary contributions (since $|\underline{\rho}-\underline{\rho}'| = R = y$):*

---

*When $\theta = \pi/2$, the pole singularities of the integrand in Eq. (70) lie on the vertical integration path in Eq. (13) through the point $\hat{w} = w - \pi/2$. No additional contribution as in (A2) need be considered, however, since $u(\pi/2 - w)$ is in this case an even function of w.

$$\hat{G}(\underline{\rho}, \underline{\rho}';t) = \frac{1}{2\pi} \frac{\sqrt{t^2 - (y/c)^2}}{t^2 - (\csc^2\alpha)(y/c)^2} \quad , \quad \theta = \frac{\pi}{2} \quad , \quad t > \frac{y}{c} \quad , \tag{74}$$

with $\hat{G} = 0$ for $t < y/c$. The first response at y occurs again at $t = y/c$, after a time interval required by a signal traveling at the speed of light to cover the distance between the source and observation points. (Note that $\hat{G} = (\hat{G}_o + \hat{G}_1)$ has no discontinuity across the impinging wave front; this behavior is a consequence of the $k^{-3/2}$ dependence in the time-harmonic high-frequency solution). A sharp increase is observed at a later time $t = (y/c)\csc\alpha$, corresponding to the signal velocity $v = c \sin\alpha$ associated with the previously discussed surface waves in the time-harmonic problem (see Sec. 5.12). Thus, the existence of surface waves on the unidirectionally conducting screen gives rise to a peak in the response function which (for $\theta = \frac{\pi}{2}$) occurs precisely after the time required for these waves to arrive at the observation point (on this non-dispersive surface, all surface waves travel with the same speed). The height of the peak is infinite when the source and observation points both lie on the surface but diminishes for other arrangements ($\theta \neq \pi/2$). A typical plot of the expression in Eq. (71c) is shown in Fig. 5, for $\alpha = 45^\circ$ and for various values of θ and (ct/R). One observes clearly the peaked response at $(ct/R) = \csc\alpha$ (dashed line) as the observation angle $\theta \to \pi/2$.

The preceding discussion suggests that the conventional surface wave in a time-harmonic field turned on suddenly at $t = 0$ is not established at a point y on the surface until after a time $t \approx (y/c)\csc\alpha$. This conjecture is verified from an examination of the transient solution corresponding to a time function

$$\begin{aligned} g(t) &= 0 \quad , \quad t < 0 \quad , \\ g(t) &= e^{j\omega t} \quad , \quad t > 0 \quad , \end{aligned} \tag{75}$$

which is obtained from Eqs. (74) and (11) for $t > y/c$ as

$$\hat{G} = \frac{1}{2\pi} \int_{y/c}^{t} e^{j\omega(t-\xi)} \frac{\sqrt{\xi^2 - (y/c)^2}}{\xi^2 - \csc^2\alpha(y/c)^2} \, d\xi \quad , \tag{76}$$

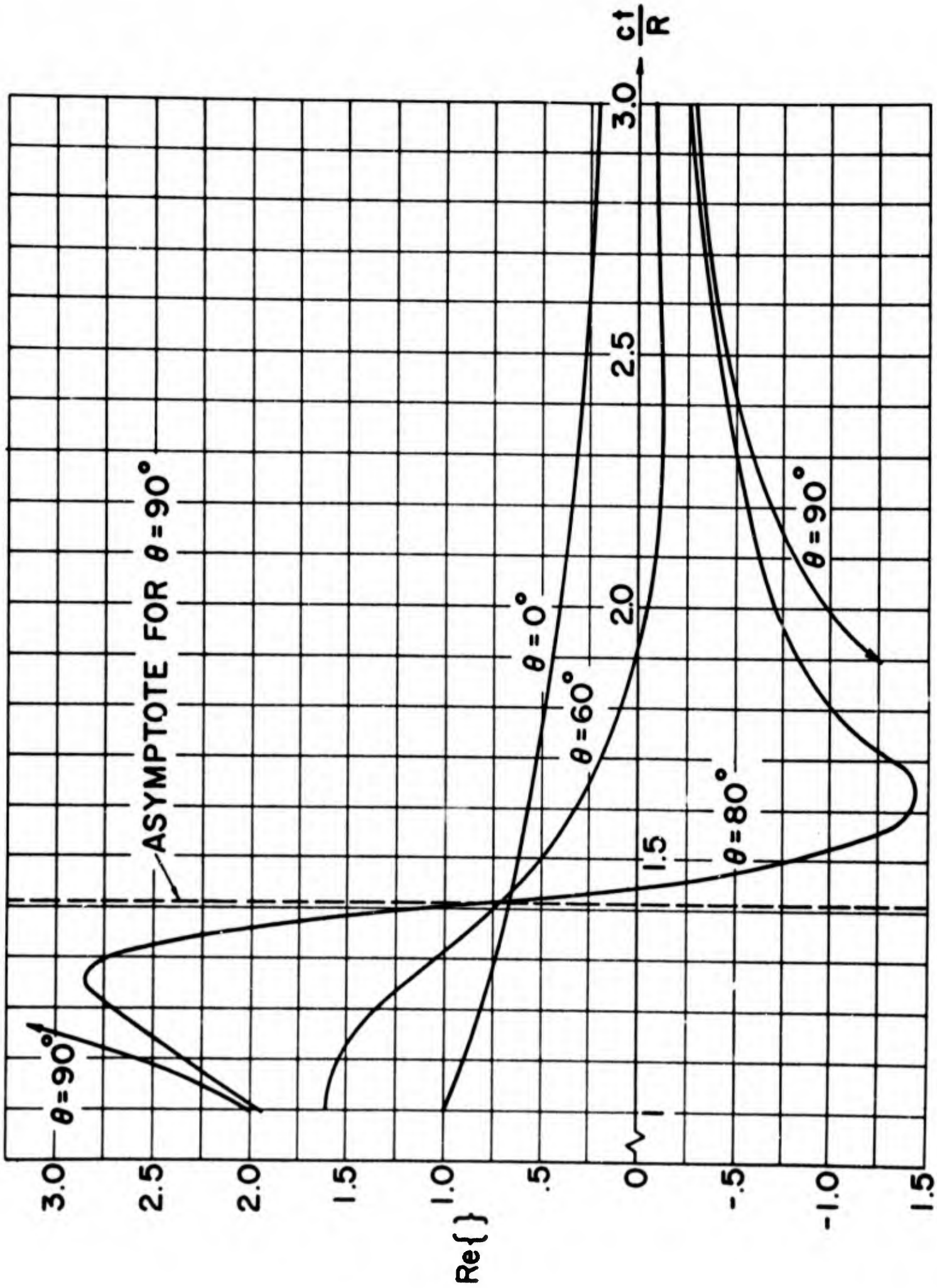

Fig. 5 - Plot of Eq. (71c)

or after changing variables to $\xi = \cosh^{-1}(\xi c/y)$,

$$\hat{G} = \frac{1}{2\pi} e^{j\omega t} \int_0^{\zeta_o} \frac{\sinh^2\zeta\, e^{-jky\cosh\zeta}}{\cosh^2\zeta - \csc^2\alpha}\, d\zeta \quad , \qquad \cosh\zeta_o = \frac{ct}{y} \quad . \tag{77}$$

Again, $\hat{G} = 0$ when $t < y/c$. For observation times $t < (y/c)\csc\alpha$, one may expand the denominator in the integrand in a series of powers of $(\cosh\zeta \sin\alpha)$ and each multiplicative factor of $\cosh\zeta$ in the integrand may be replaced by the derivative operator $-(jk)^{-1}(d/dy)$. Thus, the integral in Eq. (76) may be written as a series involving repeated spatial derivatives of

$$\int_0^{\zeta_o} e^{-jky\cosh\zeta}\, d\zeta \quad ,$$

which expression occurs in the response to a line source in free space. The series converges rapidly if $(\cosh\zeta_o \sin\alpha) \ll 1$ and the resulting field shows little evidence of the presence of a surface wave. However, for $(\cosh\zeta_o \sin\alpha) > 1$, one may write the integral in Eq. (77) as

$$\int_0^{\zeta_o} = \int_0^{\infty} - \int_{\zeta_o}^{\infty} \quad , \tag{78}$$

with the first contribution on the right-hand side* representing the steady-state solution in Eq. (70) (for $\theta = \pi/2$) and the second denoting a correction term. The steady-state response exhibits clearly the surface wave term (see Eq. (5.307)), and the correction integral

$$I = \int_{\zeta_o}^{\infty} \frac{\sinh^2\zeta\, e^{-jky\cosh\zeta}}{\cosh^2\zeta - \csc^2\alpha}\, d\zeta \le - \frac{\left(\frac{1}{k^2}\frac{d^2}{dy^2} + 1\right)}{\cosh^2\zeta_o - \csc^2\alpha} \int_{\zeta_o}^{\infty} e^{-jky\cosh\zeta}\, d\zeta \tag{79}$$

is small when $(\cosh\zeta_o \sin\alpha) \gg 1$. Thus, the surface wave appears within a time interval centered about $\cosh\zeta_o = \csc\alpha$, as anticipated.

---

*The integral is taken as the Cauchy principal value with respect to the pole at $\zeta = \cosh^{-1}\csc\alpha$. With an extension of the range of integration from $\zeta = -\infty$ to $\zeta = \infty$ and the change of variable $\zeta = (w - \pi/2)$, it is not difficult to effect a reduction to Eq. (70).

2. Half plane

The transient response of a unidirectionally conducting half plane may also be investigated readily. If the screen occupies the region $y > 0$, $z = 0$, and the line source is located at $y = a$, $z = 0$, as in Fig. 5, the fields may be calculated as before from a potential function G which now has the form (cf. Eq. (5.358)):

$$G(\underline{\rho}, \underline{\rho}'; \omega) = G_\infty(\underline{\rho}, \underline{\rho}'; \omega) + G_d(\underline{\rho}, \underline{\rho}'; \omega) \quad , \quad \underline{\rho}' \equiv (y', z') = (a, 0) \quad , \tag{80}$$

where $G_\infty(\underline{\rho}, \underline{\rho}'; \omega)$ is the potential function for the infinite screen in the preceding section,

$$G_\infty(\underline{\rho}, \underline{\rho}'; \omega) = -\frac{j}{4} H_o^{(2)}(kR) + \frac{j \cot^2 \alpha}{4\pi} \int_{\hat{P}} \frac{e^{-jkR \cos(w-\theta)}}{\csc^2 \alpha - \sin^2 w} dw \quad , \tag{80a}$$

with R and θ denoting, respectively, the distance from the source to the observation point P and the angle between R and the positive z-axis. $G_d(\underline{\rho}, \underline{\rho}'; \omega)$ expresses the perturbation introduced by the terminated screen,

$$G_d(\underline{\rho}, \underline{\rho}'; \omega) = -\frac{j}{4\pi} \frac{\cot^2 \alpha \, e^{-jka \csc \alpha}}{\sqrt{1 + \csc \alpha}} \int_{\hat{P}} \frac{\sqrt{1 - \sin w} \; e^{-jkR_1 \cos(w - \theta_1)}}{\csc^2 \alpha - \sin^2 w} dw \quad , \tag{80b}$$

where R_1 and θ_1 are the polar coordinates of the observation point measured from the edge of the screen at $y = z = 0$ (see Fig. 6).

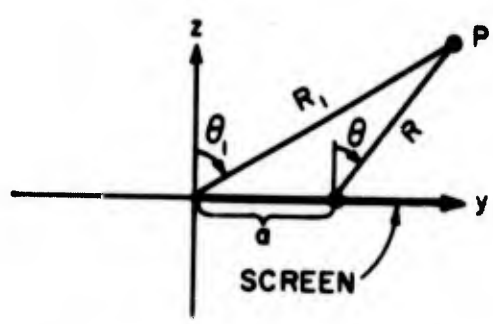

Fig. 6 - Line source and half plane

The impulse response of the infinite screen is obtained from the Laplace inversion of Eq. (80a) and has been discussed in the preceding section. The diffraction field in Eq. (80b), apart from the factor $\exp(-jka \csc \alpha)$, is also in the form shown in Eq. (12a) so that its inversion can be carried out directly. If the time function corresponding to the integral in Eq. (80b) is to be denoted by $F(t)$, then the time function corresponding to the integral multiplied by $\exp(-jka \csc \alpha)$ is $F(t-t')$, where $t' = (a/c)\csc \alpha$. From these considerations and the discussion in Section A, one obtains for the transient diffraction field,

$$0 \quad , \qquad t < \frac{R_1}{c} + t' \tag{81a}$$

$$\hat{G}_d(\underline{\rho}, \underline{\rho}';t) = \frac{\cot^2 \alpha}{\pi\sqrt{2(1+\csc \alpha)}} \; \frac{\mathrm{Re}\left\{ \dfrac{\sin\left[\dfrac{\left(\frac{\pi}{2} - \theta_1\right) - j\cosh^{-1}\frac{c(t-t')}{R_1}}{2}\right]}{\csc^2\alpha - \sin^2\left[\theta_1 + j\cosh^{-1}\frac{c(t-t')}{R_1}\right]} \right\}}{\sqrt{(t-t')^2 - (R_1/c)^2}} \quad , \quad t > \frac{R_1}{c} + t' \tag{81b}$$

where it has been recognized that $\sqrt{1 - \sin w} = \sqrt{2}\,\sin\left[(\frac{\pi}{2} - w)/2\right]$. Since $t' = (a/c)\csc \alpha$ is the time required for the surface wave field to travel from the source point on the screen to the edge, and (R_1/c) is the time of travel of a space wave from the edge to the observation point, one observes that the diffraction field for this source location is excited by the incident surface wave which is then radiated into space.

The region of validity of Eq. (81b) is confined to observation angles $|\theta_1| < \pi/2$. When $|\theta_1| = \pi/2$, the pole singularities in the integrand of Eq. (80b) lie on the integration path in Eq. (13), and the considerations in the Appendix are appropriate. Since

$$u(w) = \frac{\sqrt{2}\,\sin\left[(\frac{\pi}{2} - w)/2\right]}{\csc^2\alpha - \sin^2 w} \quad , \tag{82}$$

one has

$$u\left(\frac{\pi}{2} + w\right) = \frac{-\sqrt{2}\sin\frac{w}{2}}{\csc^2\alpha - \cos^2 w} \quad , \qquad u\left(-\frac{\pi}{2} + w\right) = \frac{\sqrt{2}\cos\frac{w}{2}}{\csc^2\alpha - \cos^2 w} \quad , \tag{83}$$

so that $u(\theta_1 + w)$ is an odd function of w when $\theta_1 = \pi/2$, but an even function when $\theta_1 = -\pi/2$. As the observation point approaches the screen, the diffracted contribution from Eq. (81b) tends to zero when $\theta_1 \to \pi/2$ with $c(t-t') \neq R_1 \csc\alpha$, but becomes infinite when $\theta_1 \to \pi/2$ with $c(t-t') = R_1 \csc\alpha$, thereby exhibiting a delta function dependence. The entire diffraction field is therefore contained in the delta function response in Eq. (A2) of Appendix A, with $w_1 = \cosh^{-1}\csc\alpha$ (note: the integration path is indented into the left half of the w-plane to avoid the poles):

$$\hat{G}_d(\underline{\rho}, \underline{\rho}';t) = \frac{\cos^2\alpha}{4(1+\sin\alpha)}\,\delta\left(t - \frac{a+y}{c}\csc\alpha\right) \quad , \qquad \theta_1 = \frac{\pi}{2} \quad . \tag{84}$$

Thus, on the screen, one observes an impulse which arrives at the observation point precisely after the time interval required by the surface waves to travel from the source to the edge and from the edge to the observation point. Unlike the cylindrical diffraction field in space which persists after the arrival of the first response, the diffraction field on the screen maintains the impulsive behavior of the excitation.

When $\theta_1 = -\pi/2$, the observation point lies on the portion of the $z = 0$ plane which is not occupied by the screen. Since $u(-(\pi/2) + w)$ is an even function of w, the impulse in Eq. (A2) is absent and $\hat{G}_d$ is given by the limiting form of Eq. (81b),

$$\hat{G}_d(\underline{\rho}, \underline{\rho}';t) = \begin{cases} 0 \quad , & t < \dfrac{|y|}{c} + t' \quad , \qquad (85a) \\[2ex] \dfrac{\cot^2\alpha}{2\pi\sqrt{(1+\csc\alpha)}}\,\dfrac{1}{\dfrac{|y|}{c}\sqrt{\dfrac{c(t-t')}{|y|} - 1}\left\{\csc^2\alpha - \left[\dfrac{c(t-t')}{y}\right]^2\right\}} \quad , & t > \dfrac{|y|}{c} + t' \quad . \qquad (85b) \end{cases}$$

where $t' = (a/c)\csc\alpha$ and the formula $\cosh(x/2) = \left[(1+\cosh x)/2\right]^{1/2}$ has been used. To this wave must be added the infinite-plane field contribution from Eq. (74).

$$\hat{G}_{\infty}(\underline{\rho}, \underline{\rho}';t) = \frac{1}{2\pi} \frac{\sqrt{t^2 - (|y| + a)^2/c^2}}{t^2 - \csc^2\alpha\left(\frac{|y| + a}{c}\right)^2}, \qquad t > \frac{|y| + a}{c} . \tag{86}$$

While both $\hat{G}_d$ and $\hat{G}_\infty$ have a singularity at $ct = (|y| + a)\csc\alpha$, the time required for the surface wave to travel from the source to the observation point along the infinite screen, one may easily verify that the singularity cancels in the sum $(\hat{G}_d + \hat{G}_\infty)$. This is in accord with the physical requirement since no surface waves can exist in the region $y < 0$.

It is of interest to explore further the different character of the surface waves radiated directly by the line source on the screen (as in Eqs. (74) and (86)) and the surface waves excited by the edge discontinuity (as in Eq. (84)). In the former case, the response is peaked about the time interval $\hat{t}$ required by a field traveling at the surface wave speed to cover the distance between the source and observation points; the increase in field strength at a given point y occurs gradually as $t \to \hat{t}$ (Fig. 7(a)). In Eq. (84), on the other hand, the response has the same impulsive dependence as the excitation (Fig. 7 (b)). This behavior may be explained after an examination of the steady-state surface wave fields which are exhibited explicitly by extracting the contributions $G_{\infty s}$ and G_{ds} from the residues at

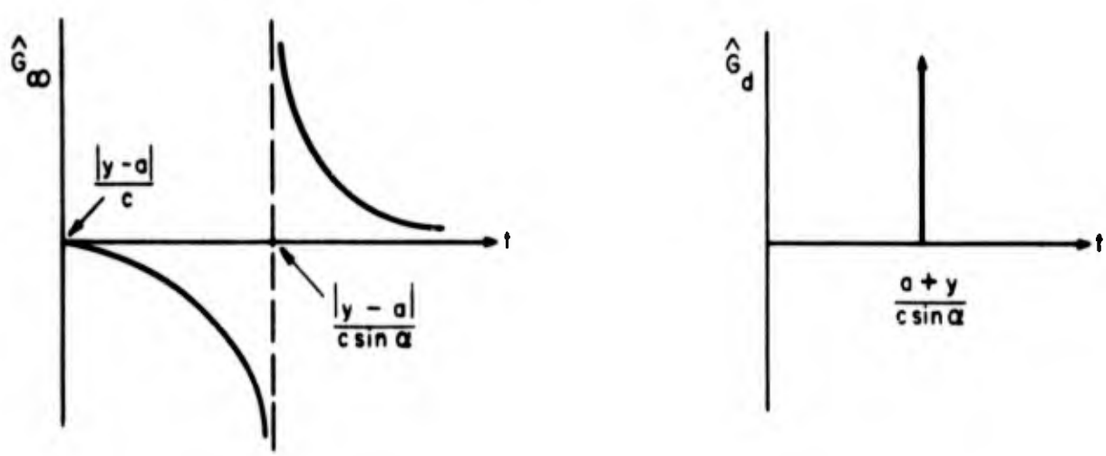

a) due to line source

b) due to edge

Fig. 7 - Transient surface wave fields on the screen

$w_p = \pi/2 + j \cosh^{-1} \csc a$ in Eqs. (80a, b):

$$G_{\infty s} = -\frac{j}{4} \cos a \, e^{k\left[-j|y-a| \csc a - |z| \cot a\right]} , \qquad k = \frac{\omega}{c} , \tag{87a}$$

$$G_{ds} = \frac{1}{4} \cos a \sqrt{\frac{\csc a - 1}{\csc a + 1}} \, e^{k\left[-j(y+a) \csc a - |z| \cot a\right]} . \tag{87b}$$

While these results differ in the k-dependent phase terms involving $|y-a|$ and $(y+a)$, respectively, and also by the real amplitude coefficient $(\csc a - 1)^{1/2} (\csc a + 1)^{-1/2}$, the significant difference between the two expressions is in the presence of the phase factor $-j = \exp(-j\pi/2)$ in Eq. (87a).

To find the real, time-dependent surface wave fields $\hat{G}_s$ excited by an impulsive source distribution $\delta(t)$, it is convenient to employ the inverse Fourier transform (see also Eq. (95))

$$\hat{G}_s = \frac{1}{2\pi} \int_{-\infty}^{\infty} G_s e^{j\omega t} d\omega = \frac{1}{2\pi}\left[\int_0^{\infty} G_s e^{j\omega t} d\omega + \int_0^{\infty} G_s^* e^{-j\omega t} d\omega \right] , \tag{88}$$

which is most useful in the second form wherein the integration extends only over positive frequencies. One easily obtains the results,

$$\hat{G}_{\infty s} = -\frac{\cos a}{4\pi} \frac{\frac{|y-a|}{c} \csc a - t}{\left(\frac{|y-a|}{c} \csc a - t\right)^2 + \left(\frac{|z|}{c} \cot a\right)^2} , \tag{89a}$$

$$\hat{G}_{ds} = \frac{\cos a}{4\pi} \sqrt{\frac{\csc a - 1}{\csc a + 1}} \frac{\frac{|z|}{c} \cot a}{\left(\frac{y+a}{c} \csc a - t\right)^2 + \left(\frac{|z|}{c} \cot a\right)^2} , \tag{89b}$$

which do not behave identically as $z \to 0$. The line-source excited contribution varies on

the screen according to

$$\hat{G}_{\infty s} = \frac{-\cos\alpha}{4\pi\left(\frac{|y-a|}{c}\csc\alpha - t\right)} \quad , \qquad |z| = 0 \quad , \tag{90a}$$

while the diffracted contribution vanishes unless $ct = (y+a)\csc\alpha$. This limiting behavior may be formulated in terms of the delta function,

$$\hat{G}_{ds} = \frac{\cos\alpha}{4}\sqrt{\frac{\csc\alpha - 1}{\csc\alpha + 1}}\,\delta\left(t - \frac{y+a}{c}\csc\alpha\right) \quad , \qquad |z| = 0 \quad , \tag{90b}$$

and yields the same expression as in Eq. (84). Thus, the phase factor $-j$ in Eq. (87a) serves to smear out the response to the impulsive excitation, whereas its form is retained for Eq. (87b).

F. Radiation from Sources in Uniform Rectilinear Motion (Cerenkov-type effects)

1. General remarks

The examples in the preceding Section have been concerned with transient processes caused by sources which are fixed in space and possess a non-harmonic variation with time. Transient fields may also be excited when the location of the source changes with time, even though the source strength itself is non-varying. The simplest class of problems in this category, involving uniform motion of an electric charge along a straight-line path, is examined in this Section. It is found that radiation occurs only when the charge speed exceeds the propagation speed of electromagnetic waves in the surrounding medium, and that the electromagnetic fields then trail behind the charge in a cone centered on the particle trajectory. The results are of interest for studies of the interaction of high-speed charged particles with material media of various types (dielectrics, plasmas, etc.), and bear on such physical applications as the absorption of protons in "swimming pool" atomic reactors, or the excitation of low-frequency noise in the earth's exosphere by streams of charges emanating from the sun.

A point charge of strength q is assumed to move with constant speed v parallel to the x-axis of a rectangular coordinate system. The current density $\hat{\underline{J}}(\underline{r}, t)$ associated with this moving charge is

$$\hat{\underline{J}}(\underline{r}, t) = \underline{x}_o qv\, \delta(x-vt)\, \delta(y-y')\, \delta(z-z') \quad ; \tag{91}$$

its Fourier spectrum function $\underline{J}(\underline{r}, \omega)$ is obtained from Eq. (1a) as

$$\underline{J}(\underline{r}, \omega) = \underline{x}_o q e^{-j(k/\beta)x} \delta(\hat{\underline{\rho}}-\hat{\underline{\rho}}') \quad , \quad \hat{\underline{\rho}} = (y, z) \quad , \quad \beta = \frac{v}{c} < 1 \quad , \quad k = \frac{\omega}{c} = \omega\sqrt{\mu_o \varepsilon_o} \quad , \tag{92}$$

where c is the speed of light in vacuum. Thus, the associated time-harmonic source distribution $\underline{J}(\underline{r},\omega)$ is a line current with a linearly varying phase, and the radiation from the moving point charge in the presence of various environments can be obtained via the inverse Fourier transformation (1b) from the time-harmonic line source solutions in Chapters V, VI, VIII or IX.

While application of the inverse Fourier transformation is essential for the determination of the real, time dependent electromagnetic fields $\hat{\underline{E}}(\underline{r}, t)$ and $\hat{\underline{H}}(\underline{r}, t)$, it can be avoided for the evaluation of the radiated energy. The Poynting vector

$$\hat{\underline{P}}(\underline{r}, t) = \hat{\underline{E}}(\underline{r}, t) \times \hat{\underline{H}}(\underline{r}, t) \tag{93}$$

represents the flow of electromagnetic field energy per unit area per unit time so that the total energy flow vector $\underline{W}(\underline{r})$ per unit area is given by

$$\underline{W}(\underline{r}) = \int_{-\infty}^{\infty} \hat{P}(\underline{r}, t)\, dt \quad . \tag{94}$$

We now substitute for $\hat{\underline{E}}$ and $\hat{\underline{H}}$ their Fourier integral representation (1b), written conveniently in terms of the complex conjugate function $f^*(\underline{r}, \omega)$ (since $\hat{f}(\underline{r}, t)$ is real, one notes from Eq. (1a) that $f(\underline{r}, -\omega) = f^*(\underline{r}, \omega)$):

$$\hat{f}(\underline{r}, t) = \frac{1}{2\pi} \int_0^{\infty} f(\underline{r}, \omega)\, e^{j\omega t}\, d\omega + \frac{1}{2\pi} \int_0^{\infty} f^*(\underline{r}, \omega)\, e^{-j\omega t}\, d\omega \quad . \tag{95}$$

Thus, upon assuming the interchangeability of the t and ω integrations,

$$4\pi^2 \underline{W}(\underline{r}) = \int_0^{\infty} d\omega \int_0^{\infty} d\omega' \Bigg\{ \underline{E}(\underline{r}, \omega) \times \underline{H}(\underline{r}, \omega') \int_{-\infty}^{\infty} e^{j(\omega+\omega')t} dt +$$

$$+ \underline{E}^*(\underline{r}, \omega) \times \underline{H}(\underline{r}, \omega') \int_{-\infty}^{\infty} e^{-j(\omega-\omega')t} dt + \underline{E}(\underline{r}, \omega) \times \underline{H}^*(\underline{r}, \omega') \int_{-\infty}^{\infty} e^{j(\omega-\omega')t} dt$$

$$+ \underline{E}^*(\underline{r}, \omega) \times \underline{H}^*(\underline{r}, \omega') \int_{-\infty}^{\infty} e^{-j(\omega+\omega')t} dt \Bigg\} \quad , \tag{96}$$

and, since $\int_{-\infty}^{\infty} e^{-j\alpha t} dt = 2\pi\, \delta(\alpha)$,

$$\underline{W}(\underline{r}) = \frac{1}{\pi} \mathrm{Re} \int_0^{\infty} \underline{P}(\underline{r}, \omega)\, d\omega \quad , \qquad \underline{P}(\underline{r}, \omega) = \underline{E}(\underline{r}, \omega) \times \underline{H}^*(\underline{r}, \omega) \quad . \tag{97}$$ *

---

*The equality of Eqs. (94) and (97) is known as Parseval's Formula.[8]

Hence,

$$\underline{W}_\omega(\underline{r}) = \frac{1}{\pi} \operatorname{Re} \underline{P}(\underline{r}, \omega)\, d\omega \quad , \tag{98}$$

represents the total energy flow per unit area in the frequency interval between ω and $(\omega + d\omega)$.

The total energy in the frequency range from ω to $(\omega + d\omega)$ flowing through a plane z = constant is given by

$$W_\omega(z) = \int_S \underline{W}_\omega(\underline{r}) \cdot \underline{z}_o \, dS \quad , \tag{99}$$

where S is the cross-section area transverse to z. Upon substituting the modal representations (see Eqs. (2.5))

$$\underline{E}_t(\underline{r}, \omega) = \sum_i V_i'(z, \omega)\, \underline{e}_i'(\underline{\rho}) + \sum_i V_i''(z, \omega)\, \underline{e}_i''(\underline{\rho}) \quad , \tag{100a}$$

$$\underline{H}_t(\underline{r}, \omega) \times \underline{z}_o = \sum_i I_i'(z, \omega)\, \underline{e}_i'(\underline{\rho}) + \sum_i I_i''(z, \omega)\, \underline{e}_i''(\underline{\rho}) \quad , \tag{100b}$$

into Eq. (99), inverting the orders of summation and integration, and recalling the orthonormality properties (2.8b) of the vector mode functions, one finds

$$W_\omega(z) = \frac{1}{\pi} \operatorname{Re}\left[\sum_i V_i'(z, \omega)\, I_i'^*(z, \omega) + \sum_i V_i''(z, \omega)\, I_i''^*(z, \omega)\right] \quad . \tag{101}$$

Thus, W_ω is given as a superposition of the individual mode powers and involves only the modal amplitudes V_i and I_i. Finally, the total energy W flowing through a plane z = constant is given by

$$W(z) = \int_S \underline{W}(\underline{r}) \cdot \underline{z}_o \, dS \quad . \tag{102}$$

2. Infinite dielectric medium

a. Circular waveguide representation

Suppose that the point charge moves in an infinite medium characterized by a real dielectric constant ϵ_1 and permeability μ_o. Because of the manifest symmetry of the electromagnetic fields about the particle trajectory, it is simplest to

employ a circular waveguide representation of the free-space region. The time-harmonic fields radiated by the line source in Eq. (92) are then inferred from the scalar Green's function (Eq. 5.65b)

$$G(\underline{r},\omega) = \frac{-j}{4} e^{-j(k/\beta)x} H_o^{(2)}(kR\gamma) \quad , \quad \gamma = \sqrt{\varepsilon - \frac{1}{\beta^2}} \quad , \quad R = |\hat{\underline{\rho}} - \hat{\underline{\rho}}'| \quad , \quad \varepsilon = \frac{\varepsilon_1}{\varepsilon_o} \quad , \tag{103}$$

to yield via Eqs. (5.66) (R and ϕ are the radial and angular coordinates in a plane transverse to the particle trajectory)

$$E_R(\underline{r},\omega) = \frac{-q}{v\varepsilon_o\varepsilon} \frac{\partial}{\partial R} G(\underline{r},\omega) \quad , \tag{104a}$$

$$E_x(\underline{r},\omega) = \frac{-q\gamma^2}{c^2\varepsilon_o\varepsilon} j\omega G(\underline{r},\omega) \quad , \tag{104b}$$

$$H_\phi(\underline{r},\omega) = -q \frac{\partial}{\partial R} G(\underline{r},\omega) \quad . \tag{104c}$$

The time dependence appropriate to these equations is $\exp(j\omega t)$, $\omega > 0$. One notes from Eq. (103) that the parameter γ determines whether the particle does, or does not, radiate electromagnetic energy. When $\varepsilon > 1/\beta^2$, where $\beta = (v/c) < 1$, γ is real and the Hankel function represents an outwardly propagating, i.e., radiating wave. The energy in this wave flows as in Fig. 5.10 along rays which make an angle $\psi = \cos^{-1}(\alpha/k\sqrt{\varepsilon})$, $\alpha = k/\beta$, with the direction of motion of the charge. The energy flow direction is therefore constant for those frequency ranges for which ε is essentially frequency independent. Since the propagation velocity of a plane wave in the medium is given by $\hat{v} = (c/\sqrt{\varepsilon})$, the range $\gamma > 0$ implies $v > \hat{v}$ so that the particle speed is greater than the propagation speed of a plane wave in the medium. Hence, the particle can excite those plane waves whose phase velocities along its direction of travel are equal to v; the propagation direction of these waves is then defined by the previously mentioned angle ψ.

When $\varepsilon < (1/\beta^2)$, $\gamma = -j|\gamma|$ is imaginary and, from Eqs. (48) and (103),

$$G(\underline{r},\omega) = \frac{1}{2\pi} e^{-j(k/\beta)x} K_o(kR|\gamma|) \quad , \quad k = \frac{\omega}{c} > 0 \quad , \tag{105}$$

so that there is no radiation. In this instance $v < \hat{v}$, and the particle cannot interact

with propagating waves in the medium. (Thus, no radiation occurs in vacuum where $\varepsilon = 1$ and $v = \beta c < c$).

The time dependent Green's function $\hat{G}(\underline{r}, t)$ is obtained from Eqs. (103) and (105) upon application of the inverse Fourier transform. For γ real, the change of variable $\omega = \bar{\omega} \exp(j\pi)$ in the second integral in (95), and use of the relation $H_o^{(1)}(x\bar{\omega}e^{j\pi}) = -H_o^{(2)}(x\bar{\omega})$, yields an expression for $\hat{G}(\underline{r}, t)$ which can be evaluated via the formula[9] (see also Eqs. (17) and (19)):

$$\int_{-\infty-jo}^{\infty} H_o^{(2)}(a\,u)\, e^{juv} du = \begin{cases} 0 & , \quad v < a \quad , \quad (106a) \\ \dfrac{4j}{\sqrt{v^2 - a^2}} & , \quad v > a \quad , \quad (106b) \end{cases}$$

so that for frequency independent ε,

$$\hat{G}(\underline{r}, t) = \begin{cases} 0 & , \quad t - \dfrac{x}{v} < \dfrac{R\gamma}{c} \quad , \quad (107a) \\ \dfrac{1}{2\pi\sqrt{\left(t - \frac{x}{v}\right)^2 - \left(\frac{R\gamma}{c}\right)^2}} & , \quad t - \dfrac{x}{v} > \dfrac{R\gamma}{c} \quad . \quad (107b) \end{cases}$$

Eqs. (107) show that the electromagnetic fields trail behind the moving charge inside a cone making an angle $\hat{\theta}$ with the x-axis as shown in Fig. 8 ; since the speed of the particle is greater than that of a wave propagating in the medium, the electromagnetic disturbance cannot run ahead of the particle. The cone is defined by the equation $(vt - x) = R\gamma\beta$ so that

$$\cot \hat{\theta} = \gamma\beta = \sqrt{\varepsilon\beta^2 - 1} \quad . \qquad (108)$$

In a coordinate system fixed to the moving charge, the electromagnetic fields are zero when $\theta > \hat{\theta}$ and are derivable from Eq. (107b) when $\theta < \hat{\theta}$. The normal direction to the conical wave front is given by the previously defined angle $\psi = (\pi/2) - \hat{\theta} = \cos^{-1}(1/\beta\sqrt{\varepsilon})$.

If γ is imaginary, the formula[10]

$$\int_{-\infty}^{\infty} K_o(a|u|) e^{juv} du = \frac{\pi}{\sqrt{v^2 + a^2}} \qquad (109)$$

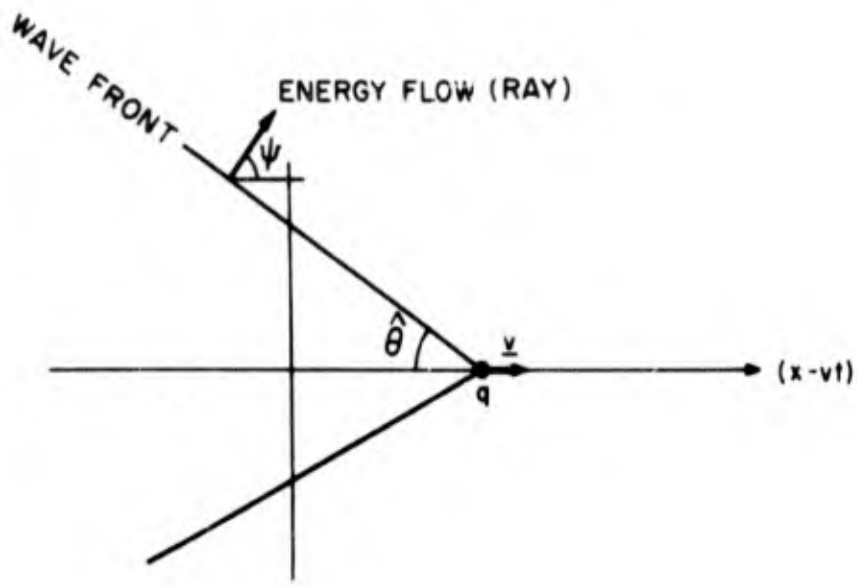

Fig. 8 - Particle moving in an infinite medium with $\varepsilon > c^2/v^2$

yields the following result for ε = constant and for all values of t,

$$\hat{G}(\underline{r}, t) = \frac{1}{4\pi\sqrt{\left(t - \frac{x}{v}\right)^2 + \left(\frac{R|\gamma|}{c}\right)^2}} \quad , \qquad |\gamma| = \sqrt{\frac{1}{\beta^2} - \varepsilon} \quad . \tag{110}$$

The associated electromagnetic fields are quasi-static and reduce to the electrostatic fields when v = 0, as noted from Eqs. (111). The magnetic field $\hat{H}_\phi$ is given via Eqs. (104) and (110) by

$$\hat{H}_\phi(\underline{r}, t) = \frac{qv}{4\pi} \frac{R}{\sqrt{1-\beta^2\varepsilon}\left[\frac{(x-vt)^2}{1-\beta^2\varepsilon} + R^2\right]^{3/2}} \quad , \qquad \beta^2\varepsilon < 1 \quad , \qquad \beta = \frac{v}{c} \quad , \tag{111a}$$

while the electric field components $\hat{E}_R$ and $\hat{E}_x$ are from Eqs. (104a, b),

$$\hat{E}_R(\underline{r}, t) = \frac{1}{\varepsilon_o \varepsilon v} \hat{H}_\phi(\underline{r}, t) = \frac{q}{4\pi\varepsilon_o\varepsilon} \frac{R}{\sqrt{1-\beta^2\varepsilon}\left[\frac{(x-vt)^2}{1-\beta^2\varepsilon} + R^2\right]^{3/2}} \quad , \tag{111b}$$

$$\hat{E}_x(\underline{r}, t) = -\frac{q\gamma^2}{c^2\varepsilon_o\varepsilon}\frac{\partial\hat{G}}{\partial t} = \frac{q}{4\pi\varepsilon_o\varepsilon}\frac{(x-vt)}{\sqrt{1-\beta^2\varepsilon}\left[\frac{(x-vt)^2}{1-\beta^2\varepsilon} + R^2\right]^{3/2}} \quad . \tag{111c}$$

Eqs. (111) can also be derived by applying a Lorentz transformation to the electrostatic particle field.[11] While for $v = 0$, $\hat{E}_x/E_R = x/R$, the effect of the motion is to shrink this ratio to $(x-vt)/R$ so that the field intensity seen by a stationary observer is no longer symmetrical about the charge.

The energy flow through a cylindrical surface surrounding the particle trajectory is readily evaluated from Eqs. (104) and (105). The total radial energy flow per unit area, in the frequency interval from ω to $(\omega + d\omega)$, is given from Eq. (98) by

$$W_\omega(\underline{r}) = -\frac{1}{\pi}\,\mathrm{Re}\left[E_x(\underline{r}, \omega)\, H_\phi^*(\underline{r}, \omega)\right] \tag{112}$$

$$= 0 \quad , \qquad \varepsilon < \frac{1}{\beta^2} \quad , \tag{112a}$$

$$= \frac{q^2k^3\gamma^3}{16\pi\omega\varepsilon_o\varepsilon}\,\mathrm{Re}\left[-jH_o^{(2)}(w)\frac{d}{dw}H_o^{(1)}(w)\right]_{w=kR\gamma} = \frac{q^2\omega\gamma^2}{8\pi^2c^2\varepsilon_o\varepsilon R} \quad , \qquad \varepsilon > \frac{1}{\beta^2} \quad . \tag{112b}$$

where use has been made of the Wronskian $J_o(x)\,N_o'(x) - N_o(x)\,J_o'(x) = 2/\pi x$. Thus, as noted previously, no radiation takes place when $\varepsilon\beta^2 < 1$. For $\varepsilon\beta^2 > 1$, the total radial energy flow per unit length (in x) in the frequency range between ω and $(\omega + d\omega)$ is from Eq. (112b)

$$W_\omega = 2\pi R\, W_\omega(R) = \frac{q^2}{4\pi\varepsilon_o c^2}\,\omega\left(1 - \frac{1}{\varepsilon\beta^2}\right) \quad , \tag{113}$$

whence one has for the total radiated energy per unit length,

$$W = \int_o^{\hat{\omega}} W_\omega\, d\omega = \frac{q^2}{4\pi\varepsilon_o c^2}\int_o^{\hat{\omega}} \omega\left(1 - \frac{1}{\varepsilon\beta^2}\right) d\omega \quad , \tag{114}$$

where $\hat{\omega}$ is the limiting frequency for which $\varepsilon(\hat{\omega})\beta^2 = 1$, i.e., $\varepsilon\beta^2 < 1$ for $\omega > \hat{\omega}$.

(If ε is assumed frequency independent, W becomes infinite; the dielectric constant of all physical media is frequency dependent and approaches that of vacuum as the frequency increases without limit; it therefore exhibits the cutoff frequency $\hat{\omega}$). These results were first derived by Frank and Tamm[12] in order to explain observed radiation from fast charged particles in media with large refractive index.

b. Rectangular waveguide representation

Alternatively, the free-space region may be regarded as a rectangular waveguide whose axis extends along the z-coordinate, with the steady-state source distribution in Eq. (92) constituting a transverse electric current which excites both E and H modes relative to the z-direction (see Sec. 5.B2). (While the rectangular waveguide description is unnecessarily complicated for the free-space configuration, it is directly pertinent to the discussion of stratified media in Sec. 2). Instead of employing the potential formulation in Eqs. (5.62) and (5.63), it will be more convenient for subsequent application of Eq. (101) to deal with the modal voltages and currents. The steady-state modal network problem is sketched in Fig. (5.9c) whence for $z > z'$,

$$V_i(z,\omega) = -\frac{Z_i(\omega)\, i_i(\omega)}{2} e^{-j\kappa_i(\omega)(z-z')} = Z_i(\omega)\, I_i(z,\omega) \quad , \tag{115}$$

where i_i, Z_i, κ_i are the current generator strength, modal characteristic impedance and propagation constant, respectively, and the dependence on ω has been indicated explicitly. The vector mode functions are (Eqs. (2.12))

$$\underline{e}_i'(\underline{\rho}) = -\frac{\nabla_t \phi_i(\underline{\rho})}{k_{ti}'} \quad , \qquad \underline{e}_i''(\underline{\rho}) = \underline{z}_o \times \frac{\nabla_t \psi_i(\underline{\rho})}{k_{ti}''} \quad . \tag{116}$$

Since all field quantities excited by the current distribution (92) will have an x-dependence given by $\exp(-jkx/\beta)$, one may define the scalar mode functions ϕ_i and ψ_i as

$$\phi_i(\underline{\rho}) = \psi_i(\underline{\rho}) = \frac{1}{\sqrt{2\pi}} e^{-j\eta y} e^{-j(k/\beta)x} \quad , \qquad -\infty < \eta < \infty \quad , \tag{116a}$$

whence,

$$k_{ti}' = k_{ti}'' = \sqrt{(k/\beta)^2 + \eta^2} \quad , \qquad \sum_i \to \int_{-\infty}^{\infty} d\eta \quad . \tag{116b}$$

Upon substituting Eqs. (92) and (116) into Eq. (2.11b), one finds, with $y' = 0$ (see also Eqs. (5.294))

$$i_i' = \frac{-jq(k/\beta)}{\sqrt{2\pi}\, k_{ti}'} \quad , \qquad i_i'' = \frac{-jq\eta}{\sqrt{2\pi}\, k_{ti}''} \quad , \tag{117a}$$

while from Eqs. (2.14),

$$Z_i' = \frac{\kappa_i'}{\omega\varepsilon_o\varepsilon} \quad , \qquad Z_i'' = \frac{\omega\mu_o}{\kappa_i''} \quad , \qquad \kappa_i' = \sqrt{k^2\varepsilon - k_{ti}'^2} = \kappa_i'' \quad . \tag{117b}$$

To calculate $W_\omega(z)$ from Eq. (101), we note first that

$$V_i' I_i'^* + V_i'' I_i''^* = \frac{Z_i'|i_i'|^2}{4} + \frac{Z_i''|i_i''|^2}{4} = \frac{q^2k^2\gamma^2}{8\pi\omega\varepsilon_o\varepsilon\kappa_i'} \quad , \tag{118}$$

where γ is defined in Eq. (103). This expression is real only when κ_i' is real so that the integration over η in Eq. (101) extends only over the interval $|\eta| \le k\gamma$:

$$W_\omega(z) = \frac{q^2k^2\gamma^2}{8\pi^2\omega\varepsilon_o\varepsilon} \int_{-k\gamma}^{k\gamma} \frac{d\eta}{\sqrt{k^2\gamma^2 - \eta^2}} = \frac{q^2k^2\gamma^2}{8\pi\omega\varepsilon_o\varepsilon} \quad . \tag{119}$$

This result represents the energy radiated through a plane at $z > z'$. By symmetry, an equal amount is radiated through a plane at $z < z'$ so that the total radiated energy (per unit length in x, in the frequency interval between ω and $d\omega$) is given by $2W_\omega(z)$, which is identical with the result in Eq. (113).

3. Two dielectric media separated by a plane interface

Next we consider the problem of radiation from a point charge in constant, straight motion parallel to an interface between two semi-infinite dielectrics characterized by the parameters $\hat{\varepsilon}_1, \mu_o$ and $\hat{\varepsilon}_2, \mu_o$, respectively. The particle trajectory is taken to coincide with the line $(y, z) = (0, z')$ as shown in Fig. 9. For practical applications, medium 1 is usually taken as vacuum ($\hat{\varepsilon}_1 = \varepsilon_o$); radiation may be produced in the denser medium 2 if $(\hat{\varepsilon}_2/\varepsilon_o)\beta^2 > 1$, in which instance the evanescent waves incident from medium 1 are converted into propagating waves in medium 2. In the analysis below, $\hat{\varepsilon}_1$ and $\hat{\varepsilon}_2$ are kept arbitrary.

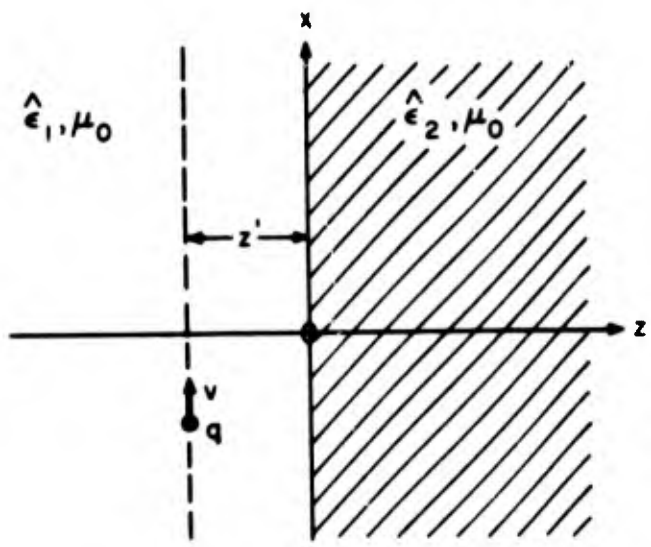

Fig. 9 - Particle moving parallel to a plane interface between two media

The associated steady-state problem, wherein the line current distribution (92) flows along the particle trajectory in Fig. 9, has been solved in a rectangular waveguide representation in Sec. 5.C3, utilizing the potential functions S' and S". For the calculation of the radiated energy, it is more convenient, however, to deal with the modal voltages and currents. The equivalent modal network problem is shown in Fig. 5.15(b), and its solution is obtained from Eqs. (5.83) or (2.42) and (2.25) as:

$$V_i(z) = -\frac{Z_{i1} i_i}{2}\left[e^{-j\kappa_{i1}|z-z'|} + \Gamma_i(0)\, e^{+j\kappa_{i1}(z+z')}\right] , \qquad z \leq 0 , \qquad (120a)$$

$$I_i(z) = -\frac{i_i}{2}\left[\mathrm{sgn}(z-z')\, e^{-j\kappa_{i1}|z-z'|} - \Gamma_i(0)\, e^{+j\kappa_{i1}(z+z')}\right] , \qquad z \leq 0 , \qquad (120b)$$

$$V_i(z) = V_i(0)\, e^{-j\kappa_{i2} z} , \qquad I_i(z) = I_i(0)\, e^{-j\kappa_{i2} z} , \qquad z \geq 0 , \qquad (120c)$$

where $\mathrm{sgn}\, x = \pm 1$, $x \gtrless 0$. Upon defining the relative dielectric constants

$$\epsilon_1 = \frac{\hat{\epsilon}_1}{\epsilon_o} , \qquad \epsilon_2 = \frac{\hat{\epsilon}_2}{\epsilon_o} , \qquad (121)$$

one may utilize directly the definitions for Z_i and κ_i given in Eq. (117b), with ε replaced by ε_1 and ε_2 in the regions $z<0$ and $z>0$, respectively. The modal current generator strengths are the same as in Eq. (117a), while the reflection coefficients are determined from Eq. (2.31) as

$$\Gamma_i(0) = \frac{Z_{i2} - Z_{i1}}{Z_{i2} + Z_{i1}} \quad . \tag{122}$$

This completes the solution of the modal network problem.

To calculate the energy flow W_ω into region 2, it is convenient to employ Eq. (120c). Since

$$V_i(0) = -\frac{Z_{i1}Z_{i2}i_i}{Z_{i1} + Z_{i2}} e^{j\kappa_{i1}z'} \quad , \qquad I_i(0) = \frac{V_i(0)}{Z_{i2}} \quad , \tag{123}$$

one finds that for imaginary κ_{i2},

$$\vec{P}_i = V_i' I_i'^* + V_i'' I_i''^* = 0 \quad , \tag{124}$$

while for (positive) real κ_{i2},

$$\vec{P}_i = \frac{q^2 \omega\mu_o \kappa_{i2}}{2\pi k_{ti}^2} \left[\frac{\kappa_{i1}^2 \varepsilon_2}{\beta^2(\varepsilon_2\kappa_{i1} + \varepsilon_1\kappa_{i2})^2} + \frac{\eta^2}{(\kappa_{i1} + \kappa_{i2})^2} \right] \quad , \qquad \kappa_{i1} \text{ real} \quad , \tag{125a}$$

$$= \frac{q^2 \omega\mu_o \kappa_{i2} e^{-2|\kappa_{i1}z'|}}{2\pi k_{ti}^2} \left[\frac{|\kappa_{i1}|^2 \varepsilon_2}{\beta^2(\varepsilon_2^2|\kappa_{i1}|^2 + \varepsilon_1^2\kappa_{i2}^2)} + \frac{\eta^2}{|\kappa_{i1}|^2 + \kappa_{i2}^2} \right] \quad , \qquad \kappa_{i1} \text{ imaginary} \quad . \tag{125b}$$

Eq. (125b) applies when $\varepsilon_2 > (1/\beta^2) > \varepsilon_1$, and this case alone is considered further. Upon substituting for $\kappa_{i1,2}$ from Eqs. (117) and (116b), one finds after some manipulation that the expression inside the square brackets in Eq. (125b) may be written in the form $\left\{ ak_{ti}^2(\eta^2 + f)\left[b(\eta^2 + g)\right]^{-1} \right\}$, where a, b, f, g are quantities independent of η, so that one obtains the following result for the real power carried in a combined E-H

mode field characterized by the index η:

$$\vec{P}_i \equiv \vec{P}_\eta = \frac{q^2\omega\mu_o}{2\pi k^2(\varepsilon_2-\varepsilon_1)}\, e^{-2\sqrt{\eta^2+k^2\left(\frac{1}{\beta^2}-\varepsilon_1\right)}\,|z'|}\sqrt{k^2\left(\varepsilon_2-\frac{1}{\beta^2}\right)-\eta^2}\;\frac{\eta^2+f}{\eta^2+g}\,, \tag{126}$$

where

$$f = \frac{k^2\varepsilon_2(1-\varepsilon_1\beta^2)}{\beta^2(\varepsilon_1+\varepsilon_2)}\,, \qquad g = \frac{k^2\left[\varepsilon_2(1-\varepsilon_1\beta^2)+\varepsilon_1\right]}{\beta^2(\varepsilon_1+\varepsilon_2)}\,, \qquad \varepsilon_2 > \frac{1}{\beta^2} > \varepsilon_1\,. \tag{126a}$$

Eq. (101) then yields the total energy flowing into the region $z>0$ in a small frequency interval centered about ω, it being recalled that the η-integration extends only over those values which render $\kappa_{1,2}$ real:[13]

$$W_\omega = \frac{1}{\pi}\int_{-\eta_o}^{\eta_o}\vec{P}_\eta\, d\eta = \frac{q^2\omega\mu_o\left(\varepsilon_2-\frac{1}{\beta^2}\right)}{2\pi^2(\varepsilon_2-\varepsilon_1)}\int_{-1}^{1}\sqrt{1-\xi^2}\;\frac{\xi^2+\hat{f}}{\xi^2+\hat{g}}\; e^{-2k|z'|\sqrt{\left(\varepsilon_2-\frac{1}{\beta^2}\right)\xi^2+\left(\frac{1}{\beta^2}-\varepsilon_1\right)}}\, d\xi\,, \tag{127}$$

where $\eta_2 = k\left[\varepsilon_2 - (1/\beta^2)\right]^{1/2}$ and the change of variable $\eta = \eta_o\xi$ has been introduced, with

$$\hat{f} = \frac{f}{k^2\left(\varepsilon_2-\frac{1}{\beta^2}\right)}\,, \qquad \hat{g} = \frac{g}{k^2\left(\varepsilon_2-\frac{1}{\beta^2}\right)}\,. \tag{127a}$$

The integral in Eq. (127) can be evaluated when the exponential term may be replaced by unity.[13] This happens when the charge trajectory lies in the interface ($z' = 0$), or less stringently, when the parameters in question are such as to make $2k|z'|\sqrt{\varepsilon_2-\varepsilon_1} \ll 1$, $k = \omega/c$. The change of variable $\zeta = \xi(\xi^2-1)^{-1/2}$ leads to

$$W_\omega = \frac{q^2\omega\mu_o\left(\varepsilon_2-\frac{1}{\beta^2}\right)}{2\pi^2(\varepsilon_2-\varepsilon_1)}\int_{-\infty}^{\infty}\frac{d\zeta}{(1+\zeta^2)^2}\;\frac{\zeta^2(1+\hat{f})+\hat{f}}{\zeta^2(1+\hat{g})+\hat{g}}\,, \tag{128}$$

which may be evaluated in terms of the residues at the poles in the upper or lower halves of the complex ζ-plane. The details are left as an exercise for the reader.

4. Anisotropic dielectric

a. Uniaxial anisotropy

The radiation characteristics of a moving charge may be altered drastically when the surrounding medium is anisotropic. The simplest situation arises when the anisotropy is uniaxial; a plasma subjected to a strong steady external magnetic field H_o may be described in this manner, and the associated tensor permittivity is given in Eq. (8.25). If the charge moves parallel to the magnetic field (this is the only feasible trajectory when $H_o >> 1$), the radiation due to the equivalent electric current distribution in Eq. (92) may be derived from a scalar Green's function which is similar to the one in Eq. (103). The details are given in Eqs. (8.46) - (8.49), and one finds that

$$E_x = \frac{jqk^2}{\omega\epsilon_o}\left(\frac{1}{\beta^2} - 1\right)G \quad , \qquad H_\phi = -q\frac{\partial G}{\partial R} \tag{129}$$

where

$$G = \frac{-j}{4}\, e^{-j(k/\beta)x}\, H_o^{(2)}\left(k\sqrt{\left(1 - \frac{1}{\beta^2}\right)\epsilon}\; R\right) \quad . \tag{129a}$$

The normalized dielectric tensor descriptive of a lossless plasma has the form

$$\underset{\sim}{\epsilon} = \underline{R}_o R_o + \underline{x}_o \underline{x}_o \epsilon \quad , \qquad \epsilon = 1 - \frac{\omega_p^2}{\omega^2} \quad , \tag{129b}$$

with $\underline{R}_o$ denoting a unit vector along the radial coordinate R transverse to the particle trajectory x. Evidently, no radiation takes place when $\epsilon > 0$ since the argument of the Hankel function is then imaginary. For $\epsilon < 0$, however, Eq. (129a) is written as (Eq. (8.49)):

$$G = \frac{j}{4}\, e^{-j(k/\beta)x}\, H_o^{(1)}\left(k\sqrt{|\epsilon|\left(\frac{1}{\beta^2} - 1\right)}\, R\right) \quad , \qquad \epsilon < 0 \quad , \tag{130}$$

and this expression, together with Eq. (129), may be employed for the calculation of the radial energy density associated with the frequency ω (Eq. (112)),

$$W_\omega(\underline{r}) = \frac{q^2\omega\mu_o}{8\pi^2 R}\left(\frac{1}{\beta^2} - 1\right) = \frac{W_\omega}{2\pi R} \quad . \tag{131}$$

W_ω, the total radial energy flow at frequency ω, is related to $W_\omega(\underline{r})$ as indicated.

The total energy radiated per unit length along the trajectory is obtained by integrating over that range of frequencies for which ϵ is negative:[14]

$$W = \int_0^{\omega_p} W_\omega \, d\omega = \frac{q^2 \mu_o \omega_p^2}{8\pi}\left(\frac{1}{\beta^2} - 1\right) \quad , \qquad \beta = \frac{v}{c} < 1 \quad . \tag{132}$$

This result implies somewhat surprisingly that slower moving particles radiate more strongly than those in rapid motion, a behavior quite different from that encountered in isotropic dielectrics.

b. Use of the refractive index diagram

The condition $\beta n > 1$, where $n = \sqrt{\epsilon}$ is the refractive index, is easily applied to the determination of the parameter range wherein radiation emanates from a charge in uniform rectilinear motion in a homogeneous isotropic dielectric, and the corresponding direction of energy transport relative to the source trajectory is specified by the angle $\psi = \cos^{-1}(1/\beta n)$. If the medium is dispersive, then $n = n(\omega)$ and different spectral components of the radiation emerge at different angles; however, n is constant at a given frequency. The latter feature does not apply in an anisotropic dielectric wherein the refractive index $n(\theta, \phi)$ is a function of the direction of propagation of a monochromatic plane wave. If the medium is a plasma subjected to an external static magnetic field, strongly dispersive characteristics in frequency are present as well, and the refractive index surfaces may take on shapes such as those shown in Fig. 9.3(a). In view of the complexity of the mathematical formulas for $n(\theta, \phi)$ in an anisotropic plasma, it is useful to mention a graphical procedure which may lend a good deal of insight into certain aspects of the Cerenkov radiation problem.[14, 15]

We proceed from the recognition that at sufficiently great distances from the source, the radiation behaves locally like a plane wave. In view of Eq. (92), each spectral component of the source (at frequency ω) has a phase dependence $\exp[-j(k/\beta)x]$, $k = \omega/c$, and this variation must likewise characterize the plane waves which carry energy into the radiation field. Since the refractive index surface defines the loci of the endpoints of the (real) phase propagation vector $\underline{k}n = \underline{x}_o \xi + \underline{y}_o \eta + \underline{z}_o \kappa$ which describes a plane wave with variation $\exp(-jn\underline{k}\cdot\underline{r})$, one observes that radiation at ω will take place only if the plane $\xi = (k/\beta)$ intersects the surface. Some further information may also be deduced from the refractive index plot: the direction of energy transport (ray direction) in a plane wave with wave vector $\underline{k}n$ is normal to the surface at the point of contact of $\underline{k}n$ (see Sec. 5, Appendix I, Chapter I) so that

the surface normals on the section $\xi = (k/\beta)$ determine the direction of the "Cerenkov ray" along which energy is carried outward from the source by a particular plane wave constituent.

The case of an isotropic medium for which the refractive index surface is the sphere n = constant serves as a simplest illustration. The ray $\underline{S}$ and the wave

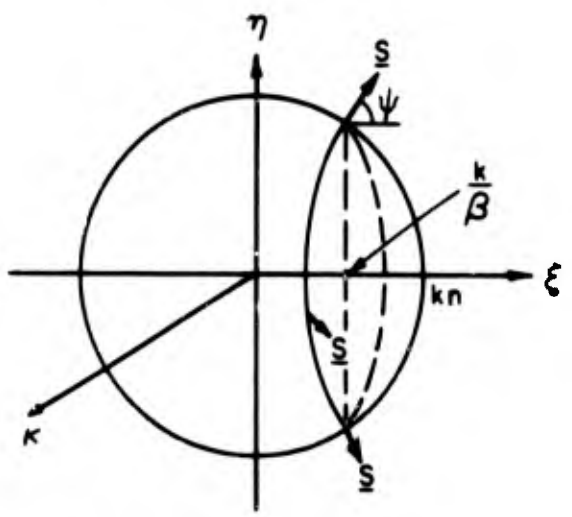

Fig. 10 - Isotropic medium

vector $\underline{k}$ are now parallel, and the construction in Fig.10 shows that radiation is possible (i.e., the plane $\xi = (k/\beta)$ intersects the sphere) when $n > (1/\beta)$ but not when $n < (1/\beta)$. Moreover, the ray vectors $\underline{S}$ are inclined at the angle $\psi = \cos^{-1}(1/\beta n)$ with the source trajectory along the x-axis. In the uniaxially anisotropic plasma described by Eq. (129b), the refractive index surface is an ellipse when $\epsilon > 0$ and a hyperbola when $\epsilon < 0$ (see Fig. 8.3, with k_o, κ, z, ρ replaced by k, ξ, x, R, respectively). Since the ellipse is confined to $|\xi| < k$, it is not intersected by the plane $\xi = (k/\beta)$, and no radiation occurs. The hyperbola, on the other hand, is intersected and gives rise to a ray whose direction may be read directly from the graph in Fig. 8.3.

These considerations remain valid when the particle trajectory is inclined with respect to the gyrotropic axis, with radiation occurring as before when the refractive index surface is intersected by the plane $\xi = k/\beta$; the direction of the ray (or rays, if multiple intersections exist) is specified by the normal to the surface on the $\xi = (k/\beta)$ contour, it being recalled that the sense of the normal is such that $\underline{k} \cdot \underline{S} > 0$ (see Appendix I, Chapter I). (An example is shown in Fig. 9.10, where the x and y axes should be interchanged to conform to the present coordinate designation.)

References

1. M. Kline and I. W. Kay, "Electromagnetic Theory and Geometrical Optics", Interscience, New York (1965). Chapters 1 and 10.

2. L. B. Felsen, "Transient Solutions for a Class of Diffraction Problems", Quart. App. Math., 23 (1965), p. 151-169.

3. A. T. deHoop and H. J. Frankena, "Radiation of Pulses Generated by a Vertical Electric Dipole above a Plane, Non-Conducting Earth", App. Sci. Res., Sec. B, 8 (1960), p. 369.

4. C. L. Pekeris and Z. Alterman, "Radiation Resulting from an Impulsive Current in a Vertical Antenna Placed on a Dielectric Ground", J. App. Phys., 28 (1957), p. 1317.

5. B. van der Pol, "On Discontinuous Electromagnetic Waves and the Occurrence of a Surface Wave", IRE Transactions on Antennas and Propagation, AP-4 (1956), p. 288.

6. F. Oberhettinger, "On the Diffraction and Reflection of Waves and Pulses by Wedges and Corners", J. Research (NBS), 61 (1958), p. 343.

7. F. G. Friedlander, "Sound Pulses", Cambridge University Press (1958), p. 120.

8. cf. A. Papoulis, "The Fourier Integral and Its Applications", McGraw Hill Book Co., New York, 1962, p. 27.

9. W. Magnus and F. Oberhettinger, "Formulas and Theorems for the Functions of Mathematical Physics", Chelsea Publishing Co., New York, 1954, p. 125.

10. Ibid., p. 116.

11. W. K. H. Panofsky and M. Phillips, "Classical Electricity and Magnetism", Addison Wesley Publishing Co., Reading, Mass., 1962, Ch. 19.

12. I. M. Frank and I. G. Tamm, Dokl. Akad. Nauk (USSR), 14 (1937), p. 109.

13. A. G. Sitenko and V. S. Talich, "Cerenkov Effect in the Motion of a Charge Above a Boundary Between Two Media", J. Tech. Phys. (Russian), 29 (1959), p. 1074-1085.

14. P. C. Clemmow, "On the Theory of Radiation from a Source in a Magneto-Ionic Medium", in "Electromagnetic Theory and Antennas", ed. by E. C. Jordan, Pergamon Press, New York, 1963, p. 471.

15. J. F. McKenzie, Phil. Trans., Roy. Soc. London, 255 (1963), p. 585-606.

Appendix A

The effect of pole singularities on the integration path

If $u(w+\varphi)$ in Eq. (13) has pole singularities on the imaginary axis in the w-plane, the inversion procedure must be modified. Of pertinence to the problems discussed in the text is the case where $u(w+\varphi)$ has simple poles at $w = \pm jw_1$, w_1 positive real, with the integration path indented around the poles into the half plane $\mathrm{Re}\, w < 0$. One obtains then instead of Eq. (14a),

$$\hat{L}(\gamma,\varphi;s) = jP \int_{\frac{\gamma}{c}}^{\infty} e^{-s\tau} \frac{u\left[\varphi + j\cosh^{-1}\left(\frac{c\tau}{\gamma}\right)\right] + u\left[\varphi - j\cosh^{-1}\left(\frac{c\tau}{\gamma}\right)\right]}{\sqrt{\tau^2 - \left(\frac{\gamma}{c}\right)^2}} d\tau$$

$$- \pi j e^{-s(\gamma/c)\cosh w_1} \left\{ (w + jw_1)\left[u(\varphi + w) - u(\varphi - w)\right] \right\}_{w = -jw_1} , \qquad \text{(A1)}$$

where P denotes the principal value of the integral with respect to the pole singularities, and the second term comprises the half residues arising from the semi-circular path segments around the poles. The inverse Laplace transform of the integral in Eq. (A1) yields the same result as in Eq. (15), while the residue contributions yield an additional delta function (note: $e^{-s\psi} = \int_0^{\infty} e^{-s\tau}\,\delta(\tau-\psi)\,d\tau$, $\psi > 0$):

$$\hat{L}(\gamma,\varphi;t)\Big|_{res} = -\pi j \left\{ (w + jw_1)\left[u(\varphi + w) - u(\varphi - w)\right] \right\}_{w = -jw_1} \delta\left(t - \frac{\gamma}{c}\cosh w_1\right) . \qquad \text{(A2)}$$

If the integration path in Eq. (13) avoids the poles through an indentation into the half plane $\mathrm{Re}\, w > 0$, the result in (A2) must be multiplied by (-1).

One observes that the residue contribution vanishes when $u(\varphi + w)$ is an even function of w.

BLANK PAGE

Unclassified

Security Classification

DOCUMENT CONTROL DATA - R&D

(Security classification of title, body of abstract and indexing annotation must be entered when the overall report is classified)

1. ORIGINATING ACTIVITY (Corporate author)

Polytechnic Institute of Brooklyn
Graduate Center, Route 110
Farmingdale, N. Y. 11735

2a. REPORT SECURITY CLASSIFICATION

Unclassified

2b. GROUP

3. REPORT TITLE

MODAL ANALYSIS AND SYNTHESIS OF ELECTROMAGNETIC FIELDS

4. DESCRIPTIVE NOTES (Type of report and inclusive dates)

Scientific Research Report

5. AUTHOR(S) (Last name, first name, initial)

Felsen, Leopold B. and Marcuvitz, Nathan

6. REPORT DATE

August 5, 1965

7a. TOTAL NO. OF PAGES

71

7b. NO. OF REFS

15

8a. CONTRACT OR GRANT NO.

AF-19(628)-4324

b. PROJECT and Task

4600-04

c. DOD Element No. 62405304

d. DOD Subelement No. 674600

9a. ORIGINATOR'S REPORT NUMBER(S)

PIBMRI-1257-65

9b. OTHER REPORT NO(S) (Any other numbers that may be assigned this report)

AFCRL-65-668

10. AVAILABILITY/LIMITATION NOTICES

Qualified requestors may obtain copies of this report from DDC. Other persons or organizations should apply to the Clearinghouse for Federal Scientific and Technical Information (CFSTI), Sills Bldg., 5285 Pt. Royal Road, Springfield, Va. 22151

11. SUPPLEMENTARY NOTES

12. SPONSORING MILITARY ACTIVITY

Hq. AFCRL, OAR (CRD)
United States Air Force
L. G. Hanscom Field, Bedford, Mass.

13. ABSTRACT

After a general discussion of non-harmonic electromagnetic processes from the viewpoint of temporal Fourier (or Laplace) analysis and synthesis, a class of problems is considered for which the transient solution may be recovered in simple form. Included in this category are pulsed point, line and plane wave sources in free space, and in the presence of a) a dielectric half-space, b) a perfectly absorbing or perfectly conducting wedge or half plane, and c) a unidirectionally conducting infinite and semi-infinite screen. Explicit expressions for the transient response, found by a systematic application of the modal procedures discussed in earlier chapters in this sequence, are interpreted in physical terms. Attention is then given to a second class of problems wherein an electric charge moves uniformly along a straight trajectory in various environments. The associated radiation is now of the Cerenkov type, and formulas for the fields as well as the radiated power are given.

DD FORM 1 JAN 64 1473

Unclassified

Security Classification

Unclassified

Security Classification

14 KEY WORDS	LINK A ROLE	LINK A WT	LINK B ROLE	LINK B WT	LINK C ROLE	LINK C WT
Radiation						
Geometrical Optics						
Transients						
Diffraction						
Guided Waves						

INSTRUCTIONS

1. **ORIGINATING ACTIVITY:** Enter the name and address of the contractor, subcontractor, grantee, Department of Defense activity or other organization *(corporate author)* issuing the report.

2a. **REPORT SECURITY CLASSIFICATION:** Enter the overall security classification of the report. Indicate whether "Restricted Data" is included. Marking is to be in accordance with appropriate security regulations.

2b. **GROUP:** Automatic downgrading is specified in DoD Directive 5200.10 and Armed Forces Industrial Manual. Enter the group number. Also, when applicable, show that optional markings have been used for Group 3 and Group 4 as authorized.

3. **REPORT TITLE:** Enter the complete report title in all capital letters. Titles in all cases should be unclassified. If a meaningful title cannot be selected without classification, show title classification in all capitals in parenthesis immediately following the title.

4. **DESCRIPTIVE NOTES:** If appropriate, enter the type of report, e.g., interim, progress, summary, annual, or final. Give the inclusive dates when a specific reporting period is covered.

5. **AUTHOR(S):** Enter the name(s) of author(s) as shown on or in the report. Enter last name, first name, middle initial. If military, show rank and branch of service. The name of the principal author is an absolute minimum requirement.

6. **REPORT DATE:** Enter the date of the report as day, month, year; or month, year. If more than one date appears on the report, use date of publication.

7a. **TOTAL NUMBER OF PAGES:** The total page count should follow normal pagination procedures, i.e., enter the number of pages containing information.

7b. **NUMBER OF REFERENCES:** Enter the total number of references cited in the report.

8a. **CONTRACT OR GRANT NUMBER:** If appropriate, enter the applicable number of the contract or grant under which the report was written.

8b, 8c, & 8d. **PROJECT NUMBER:** Enter the appropriate military department identification, such as project number, subproject number, system numbers, task number, etc.

9a. **ORIGINATOR'S REPORT NUMBER(S):** Enter the official report number by which the document will be identified and controlled by the originating activity. This number must be unique to this report.

9b. **OTHER REPORT NUMBER(S):** If the report has been assigned any other report numbers *(either by the originator or by the sponsor)*, also enter this number(s).

10. **AVAILABILITY/LIMITATION NOTICES:** Enter any limitations on further dissemination of the report, other than those imposed by security classification, using standard statements such as:

(1) "Qualified requesters may obtain copies of this report from DDC."

(2) "Foreign announcement and dissemination of this report by DDC is not authorized."

(3) "U. S. Government agencies may obtain copies of this report directly from DDC. Other qualified DDC users shall request through _____."

(4) "U. S. military agencies may obtain copies of this report directly from DDC. Other qualified users shall request through _____."

(5) "All distribution of this report is controlled. Qualified DDC users shall request through _____."

If the report has been furnished to the Office of Technical Services, Department of Commerce, for sale to the public, indicate this fact and enter the price, if known.

11. **SUPPLEMENTARY NOTES:** Use for additional explanatory notes.

12. **SPONSORING MILITARY ACTIVITY:** Enter the name of the departmental project office or laboratory sponsoring *(paying for)* the research and development. Include address.

13. **ABSTRACT:** Enter an abstract giving a brief and factual summary of the document indicative of the report, even though it may also appear elsewhere in the body of the technical report. If additional space is required, a continuation sheet shall be attached.

It is highly desirable that the abstract of classified reports be unclassified. Each paragraph of the abstract shall end with an indication of the military security classification of the information in the paragraph, represented as *(TS)*, *(S)*, *(C)*, or *(U)*.

There is no limitation on the length of the abstract. However, the suggested length is from 150 to 225 words.

14. **KEY WORDS:** Key words are technically meaningful terms or short phrases that characterize a report and may be used as index entries for cataloging the report. Key words must be selected so that no security classification is required. Identifiers, such as equipment model designation, trade name, military project code name, geographic location, may be used as key words but will be followed by an indication of technical context. The assignment of links, roles, and weights is optional.

Unclassified

Security Classification